STUDY OF BETA ADRENERGIC RECEPTORS IN THE PANCREATIC ISLETS OF METABOLIC SYNDROME INDUCED MALE C57BL/6J MICE

Final synopsis submitted to Mangalore University
for the award of the degree of

Doctor of Philosophy

in

Biotechnology

By

Vijayalakshmi G, MSc
PhD Reg. No. MU/EXB/Ph.D./CR.49/Biotech/2019-20/E.13

Dr Asha Abraham
Associate Professor & Director-LCRI
Research Supervisor

Department of Post Graduate Studies and Research in Biotechnology
St Aloysius College (Autonomous),
Mangaluru- 575 003, Karnataka, India

November 2024

Name and address of PhD student: **Vijayalakshmi G**
Research Scholar
Department of PG Studies and Research in Biotechnology, St Aloysius College (Autonomous)
Mangalore-57500
Register Number : **Ph.D Reg. No. MU/EXB/Ph.D./CR.49/Biotech/2019-20/E.13**

Name and address of Research Guide: **Dr Asha Abraham**
Associate Professor
Department of PG Studies and Research in Biotechnology, St Aloysius College (Autonomous)
Mangalore-575003

Place of Investigation: **Department of PG Studies and Research in Biotechnology, St Aloysius College (Autonomous)**
Mangalore-575003

1. INTRODUCTION

Metabolic syndrome (MetS) poses a significant global health challenge, linked to increased risks of type 2 diabetes (T2D), cardiovascular issues, and metabolic irregularities. While its exact cause remains uncertain, hypotheses point to factors like insulin resistance (IR) and stress disrupting hormonal functions (Jha et *al.,* 2023). Dysfunctional pancreatic islets, altered autonomic functions, and altered adrenergic expression in pancreatic β cells are also implicated. Beta-adrenergic receptors (β-ARs), regulating various metabolic processes, are divided into subtypes β1, β2, and β3-ARs, with their activation triggering downstream pathways crucial for metabolic homeostasis (Gorain *et al.,* 2020).

Presently, MetS lacks a definitive treatment and is addressed primarily through lifestyle adjustments, such as dietary modifications and exercise, supplemented by medications targeting specific symptoms (Aryal and Wasti, 2016). There is a serious need to formulate therapeutic approaches that address MetS holistically. While there is speculation about the potential discovery of new drugs targeting the core mechanisms of MetS, this endeavor is still in its early stages, largely due to the unclear molecular basis of the syndrome (Gupta *et al.,* 2013). Understanding of these intricate regulatory mechanisms could provide valuable insights into the underlying pathophysiology of MetS and its related complications. Additionally, lack of murine β-AR structure hampers understanding its potential functionality. Therefore, studying the structural characteristics of murine β-AR subtypes is crucial for understanding metabolic regulation, as they closely resemble human β-AR. These receptors present an

opportunity as targets for innovative drug development aimed at addressing obesity and diabetes. However, the lack of information regarding the structure of murine β-AR makes it harder to understand its functionality.

In this context, our lab developed animal models to mimic MetS in male Wistar rats (Fernandes *et al.,* 2015) and C57BL/6J mice(D'Souza and Abraham, 2014). Male C57BL/6J mice fed a high-fat simple carbohydrate (HFSC) diet displayed several MetS symptoms, such as impaired glucose tolerance, insulin resistance (IR), high blood sugar levels, abnormal lipid levels, elevated insulin levels, adrenal gland enlargement, and fatty liver (D'Souza *et al.,* 2016; D'Souza and Abraham, 2014; Swarnalatha *et al.,* 2016). These mice also had increased levels of Norepinephrine (NE) in their blood and hypothalamus (D'Souza and Abraham, 2016). The HFSC diet and its duration had specific impacts on both central and peripheral serotonergic pathways. The hypothalamic, striatal, and blood pathways were affected by the combined influence of these factors, while the urinary pathway was mainly influenced by the duration of the diet (DSouza and Abraham, 2019). Furthermore, disruptions were observed in the feedback loop of the hypothalamic–pituitary–thyroid axis (Swarnalatha *et al.,* 2018). Initial gene expression profiling of β-AR subtypes in the whole pancreas of mice identified a respective decrease and increase in *Adrb1* and *Adrb3* mRNA levels after 5 months of an HFSC diet. Additionally, pancreas of mice fed the HFSC diet exhibited diminished amounts of phosphorylated CREB and cAMP. Notably, despite the β3-AR mRNA expression, β3-AR appeared non-functional in mice with MetS (Roy, 2020).

However, additional research is necessary to validate these results and fully understand their significance. Here, we hypothesised that during MetS progression, changes in β-AR subtypes impact their coupling to adenylate cyclase, initiating downstream signalling. Given this, we investigated the levels of mRNA and protein expression for β1, β2, and β3-AR in the pancreatic islets of MetS-induced mice and examined their downstream signalling pathways to provide insights into the involvement of β-AR signalling in the development of MetS and associated metabolic disorders. A proteomic analysis of pancreatic islets of experimental group helped us to understand the dysregulated pathways. In addition, we leveraged molecular docking techniques to assess effect of NE and the efficacy of existing β-AR agonist and antagonist on β-AR subtypes in *Mus musculus*. By employing molecular docking, we aimed to gain a deeper understanding of the interactions between these ligands and receptor residues, particularly in the context of glucose-induced insulin secretion.

2. OBJECTIVES

2.1 To analyse the β-AR subtypes expression in the pancreatic islets of MetS induced male C57BL/6J mice.

i. *To induce and confirm MetS in C57BL/6J male mice by feeding HFSC diet.*
ii. *To conduct a histopathological analysis of the pancreas.*
iii. *To perform immunofluorescence analysis of the pancreas.*
iv. *To isolate pancreatic islets from mice fed HFSC and control diets.*
v. *To quantify the mRNA expression of β1, β2, and β3-AR in pancreatic islets.*
vi. *To quantify the protein expression of β1, β2, and β3-AR in pancreatic islets.*
vii. *To analyze intracellular cAMP secretion in pancreatic islets.*

2.2 To analysis the proteomic profile of the pancreatic islets from MetS induced male C57BL/6J mice.

i. *To analyze the differentially expressed proteins (DEPs) in pancreatic islets of MetS induced C57BL/6J mice.*
ii. To conduct bioinformatics analysis of differentially expressed proteins (DEPs)
iii. *To analyze functional annotation using Gene Ontology (GO) analysis*
iv. *To analyze pathway involvement through KEGG enrichment*
v. *To analyze Protein-Protein Interaction (PPI) networks*
vi. *To analyze and identify potential biomarkers*

2.3 To predict and validate the 3D structures of the β1, β2, and β3-adrenergic receptor proteins, followed by molecular docking analysis.

i. *To analyze the primary sequence of β1, β2, and β3-AR.*
ii. *To predict and validate the 3D homology model for murine β1, β2, and β3-AR protein structures using various online tools/servers.*
iii. *To perform MD simulation of β1, β2, and β3-AR.*
iv. *To analyze the interaction between β-AR agonists and antagonists with predicted β1, β2, and β3-AR protein structures using molecular docking techniques.*

2.4 To analyse the influence of Norepinephrine, β-AR agonists, and antagonists on glucose-induced insulin secretion in pancreatic islets of C57BL/6J mice.

i. *To analyze the glucose induced insulin secretion (GIIS) in pancreatic islets of C57BL/6J mice.*
ii. *To analyze the varying effects of Norepinephrine on GIIS.*
iii. *To assess the impact of β-AR agonist and antagonist on GIIS in the presence of NE.*

3. REVIEW OF LITERATURE

Metabolic syndrome (MetS) is a significant global health concern, strongly linked to an increased risk of type 2 diabetes (T2D), cardiovascular diseases, and other metabolic disturbances. Although the exact cause of MetS is still unclear, factors such as insulin resistance (IR) and hormonal imbalances are considered key contributors (Jha *et al.,* 2023). Additionally, pancreatic islet dysfunction, altered autonomic functions, and changes in adrenergic signaling in pancreatic β cells are implicated in the disease's progression. Beta-adrenergic receptors (β-ARs), which regulate various metabolic processes, are classified into three subtypes: β1, β2, and β3-ARs. Activation of these receptors triggers signaling pathways essential for maintaining metabolic homeostasis (Gorain *et al.,* 2020).

Endogenous catecholamines such as norepinephrine (NE) play a pivotal role in regulating metabolic processes including adipose tissue lipolysis, glucose homeostasis, vascular tone, and blood pressure. These processes are directly or indirectly influenced by catecholamines through β-ARs, which are G protein-coupled receptors. The β1-adrenoceptor has been highlighted for its role in energy balance regulation, with studies showing that changes in β1-AR expression in adipose tissue correlate with weight loss during calorie restriction in obese individuals (Rasmussen *et al.,* 2007). The β2-AR, widely distributed across tissues, is also crucial for mediating metabolic responses. Genetic variations in the β2-AR gene affect various physiological functions, including blood pressure regulation, adrenergic drug response, and myocardial function, positioning β2-ARs as potential therapeutic targets in MetS. Dysregulation of β3-ARs is frequently observed in obesity and insulin resistance, with reduced expression contributing to impaired lipolysis and thermogenesis, further exacerbating fat accumulation and decreased energy expenditure in MetS patients (Cero *et al.,* 2021; Lee *et al.,* 2019; Sakamoto *et al.,* 2019). Various rodent models, such as C57BL/6J mice, *ob/ob* mice, *db/db* mice, Zucker rats, and others, are widely used to study obesity and its associated metabolic disturbances. These models offer unique insights into metabolic responses, appetite regulation, leptin signaling, and genetic and environmental interactions (Chatzigeorgiou *et al.,* 2009). Specifically, the C57BL/6J mouse strain is commonly used for diet-induced obesity studies, due to its genetic predisposition to develop obesity when exposed to a high-fat diet ((Chu *et al.,* 2017). These rodent models play an essential role in advancing our understanding of metabolic disorders and the mechanisms underlying MetS.

The pancreas plays a critical role in maintaining glucose homeostasis through the coordinated actions of insulin and glucagon. Insulin promotes glucose uptake in the fed state, while glucagon facilitates glucose release during fasting (Walker *et al.,* 2011). Additionally, insulin influences glucose metabolism in the brain, particularly through the hypothalamus and brainstem (Chen *et al.,* 1975; Paranjape *et al.,* 2010; Roh *et al.,* 2016). Disruptions in glucose homeostasis lead to hyperinsulinemia, hyperglycemia, insulin resistance, impaired glucose tolerance, and pancreatic β-cell dysfunction (Prentki and Nolan, 2006; Samsonova and Zvenigorodskaia, 2011). Impaired insulin signaling results in insulin resistance, which pancreatic β-cells initially counter by increasing insulin secretion. However, this compensatory

mechanism eventually fails, leading to hyperglycemia (Kasuga, 2006). Additionally, dysfunction of α-cells can result in excessive glucagon secretion and contribute to diabetes (D'Alessio, 2011).

The sympathetic nervous system (SNS) is essential for regulating energy homeostasis through adrenergic receptors (ARs). In the liver, sympathetic activation induces glycogenolysis and gluconeogenesis *via* α1 and β2-ARs, influencing metabolism during both fed and fasted states (Carnagarin et al., 2021). In the pancreas, it stimulates glucagon secretion through β-ARs and inhibits insulin release *via* α2-ARs (Nestel *et al.,* 2017). Adipose tissue responds to SNS stimulation with lipolysis through β-ARs and inhibition by α-ARs (Karatas *et al.,* 2014), while skeletal muscle glucose uptake is facilitated by β2-ARs, and vasoconstriction of arterioles is mediated by α1-ARs. Prolonged sympathetic activation can lead to adverse metabolic outcomes. There is ongoing debate about whether sympathetic activation causes or results from metabolic alterations due to the complex interplay of factors influencing sympathetic activity and metabolic changes (Esler *et al.,* 2006). Elevated SNS activity in obesity and MetS is associated with increased urinary NE levels, muscle sympathetic nerve activity(Martinez-Sanchez *et al.,* 2022). Obese individuals often exhibit blunted sympathetic responses to physiological stimuli, contributing to inadequate thermogenesis, positive energy balance, and weight gain (Thorp and Schlaich, 2015). This blunted response can increase the risk of MetS by promoting obesity, hyperglycemia, insulin resistance, and hypertension.

The SNS plays a crucial role in regulating energy expenditure and blood pressure, with significant impacts occurring in skeletal muscle through catecholamine interactions with β2-ARs (Cero *et al.,* 2021). Catecholamines influence lipolysis in adipose tissue *via* β1, β2, β3 (stimulatory), and α2 (inhibitory) adrenoceptors, particularly during exercise and energy restriction (Jocken and Blaak, 2008). Sympathetic stimulation of β-ARs significantly affects both pre- and postprandial energy expenditure and total daily energy expenditure (Schiffelers, 2000). Genetic variations in β-adrenoceptors, such as single nucleotide polymorphisms (SNPs), have been linked to obesity and hypertension (Masuo, 2010). NE release binds to β3-ARs on brown adipose tissue, crucial for thermogenesis and energy expenditure, highlighting the importance of sympathetic innervation and adrenergic signaling in brown adipose tissue function (Cai and He, 2023; Rodrigues *et al.,* 2021).

Catecholamines, acting through β1, β2, and β3- adrenoceptor subtypes as stimulators, as well as α2-adrenoceptors as inhibitors, significantly regulate lipolysis in adipose tissue. Their role becomes particularly crucial during exercise and energy restriction periods, when there is an elevated demand for fat as a fuel source. Consequently, β-adrenoceptors play pivotal roles in energy expenditure and the regulation of body weight. Studies on DNA polymorphisms associated with these receptors have revealed correlations with MetS development. The Arg389Gly polymorphism of the ADRB1 gene displays varying frequencies of the Arg allele among different ethnic groups and is associated with obesity. The Gly16→Arg16 and Gln27→Glu27 polymorphisms of the β2-adrenergic receptor gene have been linked to metabolic syndrome in men, affecting factors like adipose tissue lipolysis, glucose homeostasis, and vascular ton (Dallongeville *et al.,* 2003). Studies have shown the strong

relationships between β3-AR polymorphisms (Trp54Arg), hypertension, metabolic syndrome, and obesity (Li *et al.,* 2021) .

In our lab, we developed a High Fat Simple Carbohydrate (HFSC) diet, modified from Fraulob et al. (2010), and administered it to one-month-old male C57BL/6J mice, resulting in dyslipidemia and T2D, effectively mimicking MetS (D'Souza and Abraham, 2014; Fraulob *et al.,* 2010) (D'Souza and Abraham, 2014). HFSC-fed C57BL/6J mice exhibited typical MetS symptoms, including impaired glucose tolerance, IR, hyperglycemia, dyslipidemia, hyperinsulinemia, adrenal gland hypertrophy, and fatty liver (Swarnalatha *et al.,* 2016; D'Souza and Abraham, 2016, 2014). Elevated NE levels were observed in both plasma and the hypothalamus (D'Souza and Abraham, 2016). The HFSC diet also impacted serotonergic pathways, affecting central and peripheral systems differently, with distinct changes in the hypothalamus, striatum, and plasma pathways (D'Souza and Abraham, 2019).

Initial gene expression studies revealed that the HFSC diet led to changes in β-AR subtypes in the pancreas. Specifically, *Adrb1* mRNA levels decreased, while *Adrb3* levels increased after five months on the diet. Additionally, phosphorylated CREB and cAMP levels were diminished in the pancreas of HFSC-fed mice. Despite an increase in *Adrb3* mRNA expression, functional β3-AR activity was not observed in these mice (Roy, 2020). However, additional research is necessary to validate these results and fully understand their significance.

The increasing prevalence of MetS highlights the need to better understand its molecular impact, especially in pancreatic islets where proteomic changes due to a HFSC diet are underexplored. Oxidative stress plays a pivotal role in β-cell dysfunction, where excess reactive oxygen species (ROS) overwhelm limited antioxidant activity, leading to damage (Asmat *et al.,* 2016; Giacco and Brownlee, 2010). This, along with dyslipidemia and obesity, accelerates β-cell destruction and insulin resistance, contributing to T2D progression (Dludla *et al.,* 2023). Additionally, impaired mitochondrial function disrupts insulin secretion and promotes apoptosis, underlining the need for deeper exploration into these mechanisms (Diane *et al.,* 2022).

β-ARs composed of 408–477 amino acids, have longer carboxy-terminal tails crucial for receptor desensitization and recycling through phosphorylation. Despite their significance in metabolic and cardiovascular functions, murine β-AR subtypes remain structurally underexplored. The human β2-AR structure, crystallized by Rasmussen *et al.* (2007), provided foundational insights into receptor-ligand dynamics, followed by the β1-AR from turkey (Warne *et al.,* 2008). Recent advancements in cryo-electron microscopy have resolved the β3-AR structure in dogs, which closely resembles human β3-AR, aiding in understanding receptor behavior (Nagiri *et al.,* 2021). However, murine models are critical for disease research, and elucidating their β-AR structures is essential to enhance drug discovery and therapeutic strategies.

Insulin secretion by pancreatic beta cells is tightly regulated by several factors, with glucose acting as the primary driver. Key mechanisms, including ATP-sensitive potassium channels,

hormones, nutrients, and neural inputs, control insulin release to maintain glucose homeostasis, a critical process for understanding MetS pathophysiology (Fu *et al.,* 2013; Kojima *et al.,* 2017). NE plays a significant role in modulating glucose-induced insulin secretion, with distinct inhibitory effects observed in rodent islets, such as activation of K^+ channels, inhibition of adenylyl cyclase, and disruption of exocytosis (Straub and Sharp, 2012). NE's inhibition of insulin secretion is mediated by Gα subunits and downstream signaling pathways, interfering with glucose-induced exocytosis.

Adrenergic receptors mediate catecholamine effects like NE and epinephrine in various physiological processes (Borelli and Gagliardino, 2001). β-ARs are particularly involved in regulating insulin release. β-AR agonists such as NE and isoproterenol stimulate insulin secretion, while antagonists like propranolol inhibit it. However, the β2-adrenergic agonist clenbuterol was ineffective in stimulating insulin secretion in isolated rat islets, indicating differential roles for β-AR subtypes in insulin release (Lacey *et al.,* 1990). Despite substantial research, the precise role of NE and β-AR interactions in modulating GIIS remains incompletely understood.

Overall, the role of β-ARs in pancreatic function, particularly under the influence of a HFSC diet, remains an underexplored area in metabolic research. Understanding how β-AR signaling affects MetS pathophysiology is crucial, yet significant gaps exist regarding how β-AR subtypes and downstream signaling in pancreatic islets respond to HFSC-induced metabolic stress. Additionally, proteomic changes within islets under such dietary conditions are poorly understood and may play a key role in linking MetS to severe pancreatic dysfunction, followed by other disease pathophysiology. While homology models and *in silico* methods hold promise for predicting receptor-ligand interactions, more precise 3D structural predictions of murine β-ARs are needed for developing receptor-targeted therapies. Furthermore, the role of neurotransmitters like norepinephrine in modulating glucose-induced insulin secretion in MetS conditions also requires further investigation. Addressing these knowledge gaps is essential for advancing therapeutic strategies aimed at treating metabolic disorders and improving pancreatic health.

4. MATERIALS AND METHODS

4.1 ANALYSIS OF THE β1, β2 and β3-AR EXPRESSION IN METS INDUCED MICE.

4.1.1. Induction of MetS

Healthy male C57BL/6J mice, obtained from an authorized vendor, were housed in a controlled environment (25 ± 2°C, 12-h light/dark cycle) following protocols approved by the Committee for Control and Supervision of Experiments on Animals, India. The Institutional Animal Ethics Committee of St Aloysius College (Autonomous) Mangalore, India, approved the experiments (Sanction No: SAC/IAEC/05/2019, 28 January 2019). One-month-old male C57BL/6J mice

weighing between 18 and 20 g were randomly assigned to control (n=10) or HFSC (n=10) groups. The control group received a standard diet, while the HFSC group received a specially formulated high-fat, high-sucrose (HFSC) diet. Both groups were provided with 5 g/day of their respective diets, in compliance with Indian National Science Academy regulations (2000), with ad libitum access to water. These conditions were maintained for 150 days with regular monitoring of body weight (BW) and blood glucose levels. The control diet consisted of wheat flour (79% [w/w]), spray-dried infant milk formula (Amul, Anand, India; 16% [w/w]), and soybean oil (4.67% [v/w]), while the HFSC diet contained porcine fat (13% [w/w]), sucrose (10% [w/w]), corn starch (7% [w/w]), and spray-dried infant milk formula (Amul; 70% [w/w]). The total energy contents of the control and HFSC diets were 3583 and 5065 kcal/kg, respectively (D'Souza *et al.,* 2016).

4.1.2 MetS confirmation

MetS was confirmed using morphometric measurements, blood glucose levels, and lipid profiles. Body weight (BW) and ano-nasal length (ANL) were measured monthly. The Lee index was calculated for both groups using this formula: Lee index = BW (g) / (ANL [cm])^2. Blood samples were collected on days 30, 60, 90, 120, and 150 by tail vein bleeding. Blood glucose levels were measured utilizing a glucometer and blood glucose test strips. The serum was analysed for levels of total cholesterol (TC), triglycerides (TG), high-density lipoprotein (HDL), and low-density lipoprotein (LDL) using SD Lipidocare lipid test strips (SD Biosensor).

4.1.3 Isolation of the pancreas and histological analysis

The control and HFSC-fed mice were fasted overnight before euthanizing via cervical dislocation on day 150 of the experiment. Pancreas retrieval involved dissection using sterile blades and forceps, followed by storage in 10% formalin for 8 hours for subsequent histological analyses. H&E staining was used to analyze pancreatic islet morphology. Tissue sections were deparaffinized, hydrated, stained with Harris haematoxylin and eosin Y solution, washed, dehydrated, and mounted. Slides were observed under a BX 41 microscope with a CCD camera and analyzed using ProgRes CapturePro 2.8.8 software.

4.1.4 Immunofluorescence analysis of pancreas

Pancreatic tissues from HFSC-fed and control mice were processed as described above. The tissue sections were subjected to citrate-buffered antigen retrieval. Immunofluorescence staining was subsequently performed according to a standard protocol (Zaqout *et al.,* 2020). The sections were treated individually with primary rabbit polyclonal antibodies against β1-AR (Invitrogen, USA), β2-AR (Invitrogen), β3-AR (Bioss, USA), and β-actin (Invitrogen) (as a loading control), followed by overnight incubation at 4 °C. Subsequently, the sections were treated with goat anti-rabbit IgG (H+L) cross-adsorbed DyLight488 secondary antibody (Invitrogen)for 120 min at room temperature (RT; 24°C) in the dark. The slides were observed under a fluorescence microscope (Olympus), and images were captured using a CCD camera (Jenoptic) to precisely quantify fluorescently active cells in the samples.

4.1.5 Isolation of pancreatic islets

The pancreatic islets from the experimental groups were isolated using Collagenase digestion (Sigma-Aldrich, USA). The dissected pancreas was treated with collagenase type IV at 1

mg/mL in ice-cold HBSS and incubated at 37 ± 2°C with shaking for 15 minutes. After digestion, the suspension was filtered and centrifuged, and the resulting islet suspension was selected for further analysis. Pancreatic islet quality was assessed using dithiozone staining (Himedia, India), which stains their Zn-enriched region. The Zn-enriched region in pancreatic islets is vital for insulin storage and secretion, serving as a critical cofactor for insulin crystallization within secretory granules, thus impacting insulin release and glucose homeostasis.

4.1.6 Total RNA Isolation, quantification and cDNA synthesis

Total RNA was extracted from isolated pancreatic islet of the experimental groups using TRI reagent (GeNei, India) according to the manufacturer's protocol. The quantification and purity of the isolated total RNA was determined using Spectrophotometer (Nano Drop ND-2000c by Thermo Fisher Scientific, USA). 2.0µg of total RNA with purity between 1.8 and 2.0 was reverse 5 transcribed using a combination of random hexamers and oligo dT (18mer) and enzyme MMuLV reverse transcriptase (GeNei) after Dnase I treatment (Sigma-Aldrich).

4.1.7 Primer designing and standardization

Primers for *Adrb1, Adrb2, Adrb3*, and *Actb* were designed using Primer 3 Plus. *In-silico* PCR was conducted using online tools such as UCSC *In-silico* PCR and Primer-BLAST to verify primer specificity. The designed primers were custom synthesized by Sigma and standardized to find the optimum annealing temperature using gradient PCR method.

4.1.8 Determination of β-AR-subtype gene expression using qRT-PCR

Quantitative real time PCR (qRTPCR) was performed using StepOne Real-Time PCR (Applied Biosystem. SYBR green chemistry using Power SYBR® Green Master mix was employed for qRTPCR. β actin was used as the reference gene. Gene expression was determined by comparative CT method (Schmittgen and Livak 2008).

4.1.9 Determination of β-AR-subtype protein expression using western blotting

Total proteins from isolated pancreatic islets were extracted using RIPA lysis buffer (Thermo Fisher Scientific) with protease and phosphatase inhibitor cocktail as per the manufacturer's instructions. Protein quantification was done using a Pierce BCA kit (Thermo Fisher Scientific). Protein samples were preheated with 2× Laemmli buffer (Sigma-Aldrich) and separated using SDS-PAGE. Electroblotting onto polyvinylidene difluoride membranes (Merck Millipore) was performed at 60 V for 90 min. Membranes were blocked with 5% non-fat milk and washed with Tris-buffered saline containing 1% Tween-20 Sigma-Aldrich. Incubation with primary rabbit polyclonal antibodies against β1-AR (Invitrogen), β2-AR (Invitrogen), β3-AR (Bioss), and β-actin (Invitrogen), was done overnight at 4°C. Following this, membranes were exposed to a goat anti-rabbit IgH (H+L) cross-adsorbed DyLight488 (Invitrogen), secondary antibody. Blots were imaged using a Gel Doc XR+ (Bio-Rad) with a DyLight488 filter and quantified using Bio-Rad Image Lab. Protein expression was normalized to the loading control β-actin.

4.1.10 Determination of intracellular cAMP using ELISA

The isolated pancreatic islets were rinsed with ice-cold PBS. Islets were homogenized using RIPA lysis buffer, and the supernatant was collected after centrifugation. Intracellular cAMP

concentrations were determined using an ELISA kit (RayBiotech, USA)following the manufacturer's instructions. Absorbance was measured at 450 nm, and changes in cAMP concentration were calculated as A/A0, where A represents the cAMP concentration for the HFSC diet group and A0 represents the control group without treatment.

4.1.11 Statistical analysis

Data are expressed as mean ± SD. Statistical analyses were performed using GraphPad Prism version 10. Multiple paired *t*-tests were employed to assess temporal changes for the Lee index, preliminary screening. Independent samples *t*-test was used to analyse gene expression, protein expression and cAMP secretion. Levels of statistical significance were set at $p^{***} < 0.001$, $p^{**} < 0.01$ and $p^{*} < 0.05$.

4.2 PROTEOMIC PROFILING OF PANCREATIC ISLETS IN C57BL/6J MICE: IDENTIFICATION OF DIFFERENTIALLY EXPRESSED PROTEINS (DEPS)

4.2.1 Induction of MetS

MetS was induced in male C57BL/6J mice as detailed in section 4.1.1.

4.2.2 Preparation of pancreatic islets

Pancreatic islet was isolated from experimental group as detailed in section 4.1.5.

4.2.3 Extraction of Mass Spectrometry-suitable protein using Rapigest

To extract proteins from pancreatic islets, the islets were washed with ice-cold PBS, centrifuged, and the resulting pellet transferred to a fresh tube. After a final wash, the pellet was mixed with Rapigest extraction buffer (Waters, India) and protease inhibitors and incubated. Freeze-thaw cycles were performed using liquid nitrogen, followed by centrifugation to collect the protein-containing supernatant. This protein extract was desalted using Amicon Ultra filters (Sigma-Aldrich), quantified with a BCA kit, and adjusted to a concentration of 1 mg/mL.

4.2.4 Trypsin digestion

The protein samples from both the HFSC and control groups were first reduced using 100 mM 1,4-Dithiothreitol (Sigma-Aldrich) and then alkylated with 200 mM iodoacetamide (Sigma-Aldrich). Following this, an overnight digestion was performed using MS-grade trypsin (Sigma-Aldrich).

4.2.5 Liquid Chromatography and Mass Spectrometry

Liquid chromatography analyses were conducted using a nanoACQUITY UPLC® system (Waters) with MassLynx4.1 software, employing a two-solvent system and a Symmetry® C18

column for trapping followed by a 75 µm × 200 mm HSS T3 C18 column for separation. The flow rate was 300 nL/min at 35°C, with analyses performed in reverse phase mode and a 90-minute gradient run time. Mass spectrometry was performed on a Synapt G2 High Definition MS™ System with sodium iodide calibration and electrospray ionization (ESI) in positive polarity. Leucine encephalin was used for online mass correction. Data acquisition was in resolution mode with collision energy ranging from 20 eV to 45 eV.4.2.4 Data Analysis of Proteomics Data. Progenesis QI software was used for proteomics analysis with *Mus musculus* protein database UniProt entries. Default settings were followed, including peak picking with a 20-ion charge limit and a 4% false discovery rate. Cysteine carbamidomethylation and methionine oxidation were set as modifications, with one missed cleavage allowed. Normalized intensity values from three replicates were used for label-free quantification.

4.2.6 Identification of DEPs and Bioinformatics analysis

Proteomics data analysis was performed using MetaboAnalyst 6.0, employing median normalization to ensure consistency. Differentially expressed proteins (DEPs) were identified using a volcano plot with thresholds set at a 1.5-fold change and a p-value < 0.05, and the results were visualized using heatmaps. For functional annotation, Gene Ontology (GO) and Kyoto Encyclopedia of Genes and Genomes (KEGG) enrichment analyses were conducted using ShinyGO, an R-based tool accessible online, with significant pathways filtered by an adjusted p-value < 0.05. To further explore protein interactions, the STRING database was utilized to integrate known and predicted protein-protein interactions, revealing potential functional linkages among the DEPs.

4.3 HOMOLOGY MODELLING OF MURINE β1-AR, β2-AR, and β3-AR PROTEIN STRUCTURE AND MOLECULAR DOCKING

4.3.1 Preliminary sequence analysis and TM helix prediction

The β1, β2 and β3-AR amino acid sequence were retrieved from NCBI. Key physicochemical properties including molecular weight, isoelectric point, extinction coefficient, aliphatic index, and charge distribution were assessed using ExPASy's ProtParam server. Moreover, the server was utilized to determine the GRAVY parameters for the β-AR subtypes protein in *Mus musculus.* Transmembrane region was predicted using TMHMM.

4.3.2 Prediction and validation of protein structures

The 3D structures for murine β1, β2, and β3-AR predicted using Phyre 2, SWISS MODEL, i-TASSER and AlphaFold. The stereochemical analysis was performed using SAVES. The structures were refined, and energy minimized using ModRefiner. To validate the refined structures, we utilized the SAVES v6.0 suite, which includes various validation modules such as ERRAT, VERIFY 3D, and PROCHECK. The binding sites for the predicted structures were identified using CASTp.

4.3.3 Molecular dynamic simulation

Molecular dynamics (MD) simulations were performed using GROMACS on the WEBGRO server, with the GROMOS96 43a1 forcefield for atomic and molecular interactions. The SPC water model was used, and a triclinic box type was chosen to fit the system's geometry. Sodium

chloride (NaCl) at 0.15M concentration was added for system neutrality. Prior to production simulations, energy minimization was conducted with the Steepest Descent integrator for 5000 steps. Equilibration and MD runs were carried out using NVT and NPT ensembles at 300 K and 1.0 bar. The Leap-frog integrator was applied for equation integration, with a total simulation time of 50 ns and approximately 1000 frames collected for analysis.

4.3.4 Molecular docking

The binding interactions between Norepinephrine, CL316 243, Propranolol, L748337 and predefined binding sites within target protein structures. Prior to docking, files were prepared using AutoDock, involving removal of water molecules, addition of polar hydrogen atoms, and charge assignment using the Gasteiger method. Default energy range of 4 was maintained throughout the study. Ligand binding affinity, expressed in kcal/mol, was indicated by negative scores. Predicted binding modes with the most favorable Gibbs free energy and preferred clusters were examined. Initially, binding pockets were identified using AutoGrid to ensure coverage of key residues essential for ligand recognition and binding. Subsequently, molecular docking simulations were conducted using AutoDock Vina, employing prepared ligand structures and refined protein targets. Outcomes were visualized using the academic version of the *Schrödinger Maestro suite.*

4.4 INVESTIGATING THE EFFECTS OF NE, β-AR AGONISTS, AND ANTAGONISTS ON GLUCOSE-INDUCED INSULIN SECRETION IN MOUSE PANCREATIC ISLETS

4.4.1 Preparation of pancreatic islets

Pancreatic islet was isolated from experimental group as detailed in section 4.1.5.

4. 4.1 Glucose-Induced Insulin Secretion and ELISA

For glucose-induced insulin secretion and ELISA, isolated pancreatic islets were rinsed with Krebs-Ringer solution and diluted to a concentration of 90-100 islets per 10µl of media. The diluted islet suspension underwent incubation at high (20mM) and low (5mM) concentrations of D-glucose, with and without NE (1nm, 10nm, 100nm, 1000nm, 10000nm) (Sigma-Aldrich), propranolol (Sigma-Aldrich), CL316, 243 (Sigma-Aldrich), and L-748,337 (Tocris Biotech, USA) for 2 hours at 37°C. After incubation, secreted insulin were centrifuged, and the supernatant was collected for quantification using a mouse insulin ELISA kit (RayBio® mouse Insulin ELISA kit, USA) according to the manufacturer's protocol.

4.4.2 Data Analysis

The data is presented as Mean ± SD (standard deviation). Statistical significance was assessed using Analysis of Variance (ANOVA) conducted with GraphPad Prism 10.1. Levels of statistical significance were set at $p< 0.001$, $p< 0.01$ and $p< 0.05$.

5. RESULTS AND DISCUSSION

5.1 ANALYSIS OF β-AR SUBTYPES EXPRESSION AND cAMP IN PANCREATIC ISLETS OF C57BL/6J MICE

5.1.1 Confirmation of MetS

As MetS progressed, BW increased significantly in the HFSC group compared to the control group at 30, 60, 120, and 150 days ($p < 0.05$, $p < 0.01$, $p < 0.01$, and $p < 0.001$, respectively) (Figure 1A), indicating the hallmark of MetS. The Lee index, used to assess obesity severity, significantly increased in the HFSC group after 60 days compared to the control ($p < 0.01$) (Figure 1B). Fasting serum blood glucose levels significantly increased in the HFSC group between days 30 and 60 ($p < 0.01$), remaining elevated until day 150 (Figure 1C). TG levels significantly increased in the HFSC group between days 30 and 60 ($p < 0.01$) and days 120 and 150 ($p < 0.001$) (Figure 1D). Fasting serum TC levels increased rapidly in the HFSC group at 30 and 60 days ($p < 0.01$) and 120 and 150 days ($p < 0.001$) (Figure 1E). Fasting plasma LDL levels were significantly higher in the HFSC group at days 120 and 150 ($p < 0.001$) (Figure 1F), while fasting plasma HDL levels significantly decreased between days 120 and 150 ($p < 0.01$) in the HFSC group (Figure 1G). This agrees with previous report (Song *et al.,* 2017; Bravo *et al.,* 2014; Botezelli *et al.,* 2010; Hariri *et al.,* 2010; Higa *et al.,* 2014; Vekic *et al.,* 2019; Martins *et al.,* 2022).

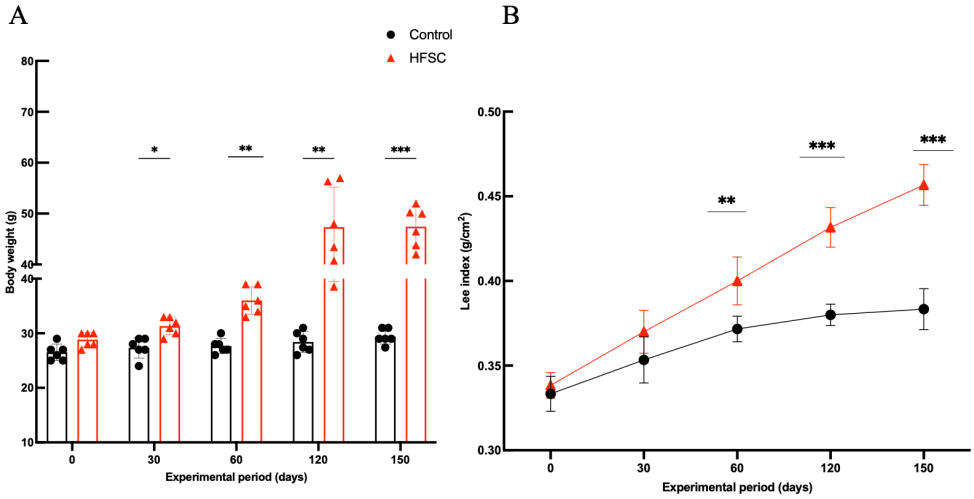

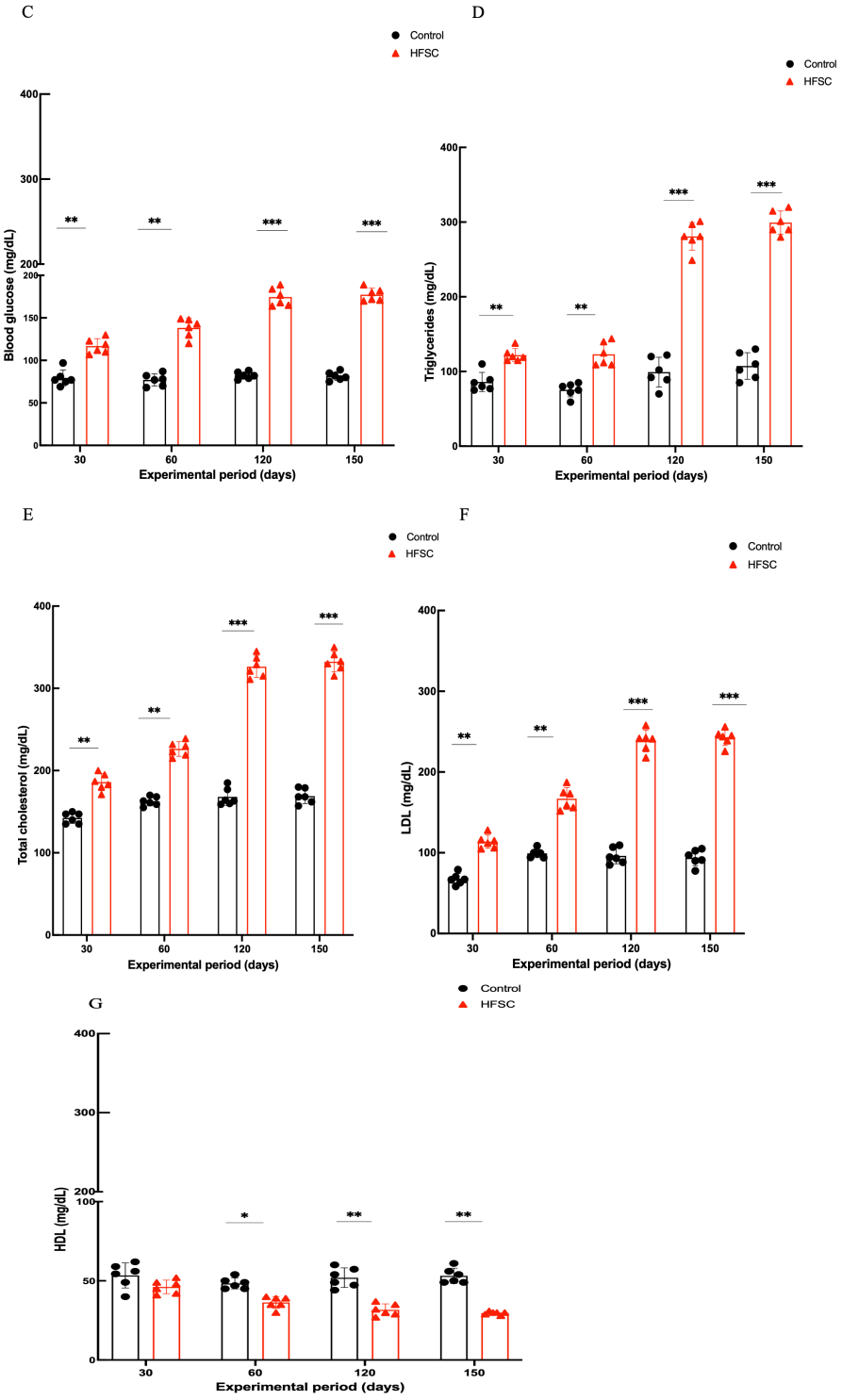

Figure 1. Dietary impact on body weight, Lee index, blood glucose, and lipid profiles in male C57BL/6J mice.

*Effect of diet on the body weight (A), Lee index (B), blood glucose (C), and lipid profiles in male C57BL/6J mice. The control and HFSC data represent measurements for each metabolic marker at different intervals. Levels of triglycerides (D), total cholesterol (E), LDL (F), HDL (G). Data are expressed as mean ± standard deviation (SD) for six independent values. ***p < 0.001, **p < 0.01, *p < 0.05 compared with the control. HDL, high-density lipoprotein; HFSC, high fat simple carbohydrate; LDL, low-density lipoprotein.*

5.1.2 Analysis of pancreas histology and quality

H&E staining revealed distinct differences between the pancreases of the control and HFSC groups. In the control group, pancreatic islets appeared normal (Figure 2A and 2C), while the HFSC group showed inflammation in the islets, enlarged islets, and a higher islet count (Figure 2B). Similar findings were reported in mice fed a high-fat diet (Fraulob et al., 2010). Additionally, the HFSC group exhibited disruptions in the morphology of pancreatic acinar cells, which are responsible for producing and secreting digestive enzymes (Figure 2B). These cells appeared hypertrophied with irregular shapes and sizes, suggesting that the HFSC diet may have negatively affected acinar cell structure and function (Figure 2D). Additionally, mice fed an HFSC diet developed pancreatic steatosis (Figure 2E). Pancreatic islets from the control group showed a normal structure with intact and healthy islet cells (Figure 3A). In contrast, islets from the HFSC group displayed signs of inflammation, with broken structures (Figure 3B).

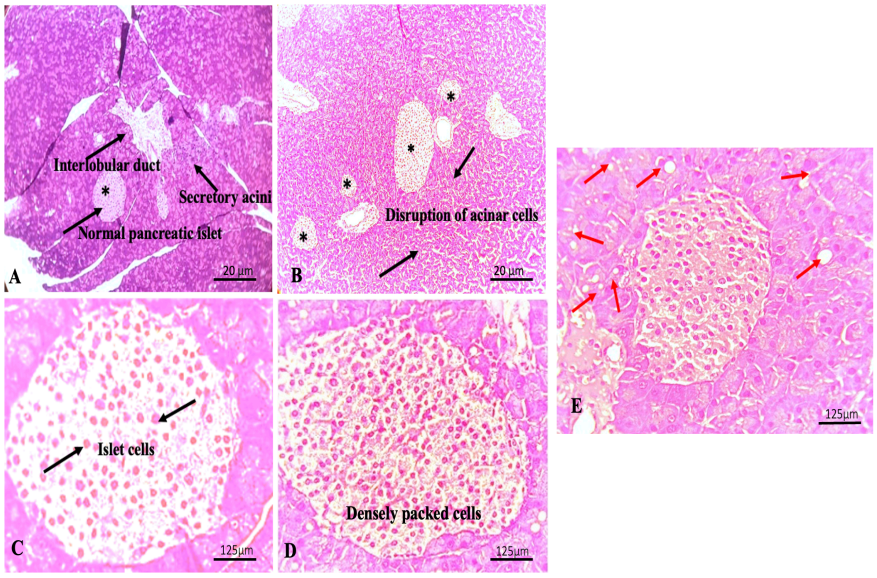

Figure 2. Histological examination of the pancreas from experimental mice group.

*A) H&E staining for mice fed the control diet showing normal pancreas tissue with healthy islets under 100× resolution. B) H&E staining for mice fed the HFSC diet showing enlarged pancreatic islets and disrupted acinar cells. C) Control diet fed mice showing intact islets at 400X resolution. D) HFSC fed the mice showing islet densely packed cells. E) Development of Pancreatic steatosis in mice fed HFSC diet (red arrow indicated the fat accumulation in the exocrine pancreas). * indicates the pancreatic islets.*

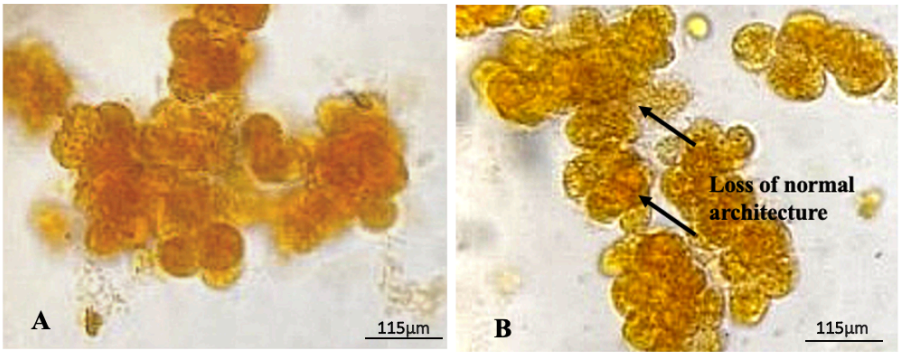

Figure 3. DTZ staining of pancreatic islets.

A) DTZ staining for mice fed with control diet showing intact islets. B) DTZ staining of HFSC-fed mice showing the loss of normal architecture. Images were acquired on an inverted microscope at 400X magnification.

5.1.3 Primer designing and standardisation

The qPCR specific primers (Table. 1)were designed using Primer 3 Plus software.

Table. 1 Forward and backward primers for *Adrb1*, *Adrb2,* and *Adrb3*

Gene	Forward primer	Reverse Primer
Adrb1	5′-CGCGAGCAGAAGGCGCTCAAG-3′	5′-GAGTTGGCGTAGCCCAGCCAGT-3′
Adrb2	5′-CGTCACTCAGGAACGGGACGAAGC-3′	5′-GACTGGCCCCAAACGGCACC-3′
Adrb3	5′-GGCAGATGCCGAGGCACAGGA-3′	5′-GGACGGAGAGCGCGACGGA-3′
Actb	5′-CGTGCGTGACATCAAAGAGAA-3′	5′-CAAGAAGGAAGGCTGGAAAGA-3′

5.1.4 mRNA expression of *Adrb1*, *Adrb2,* and *Adrb3* in the pancreatic islet

The relative expression of *Adrb1* was significantly upregulated ($p < 0.001$) in the HFSC group compared to that in the control group. In contrast, *Adrb2* expression was downregulated in the HFSC-fed group. Specifically, the control group exhibited a significant increase in relative expression ($p < 0.01$), whereas the HFSC group exhibited decreased relative expression. Hence, an HFSC diet could impact *Adrb1 and Adrb2* expression. Moreover, the relative expression of *Adrb3* did not significantly alter the pancreatic islets of the HFSC group compared to those of the control group (Figure 4).

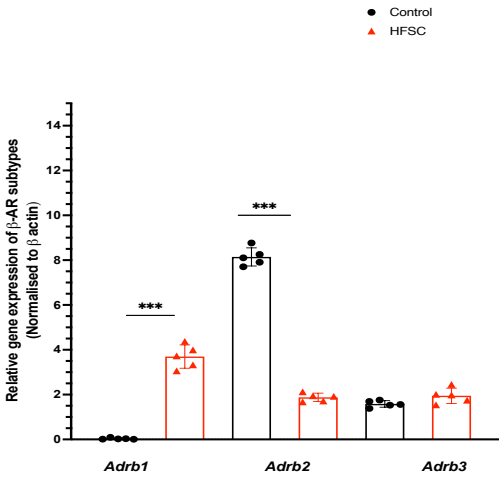

Figure 4. Effect of diet on relative mRNA expression for β-adrenergic receptor (β-AR) subtypes assessed using quantitative real-time polymerase chain reaction.
*Data are expressed as mean ± standard deviation (SD) for five independent values. ***p < 0.001 compared with the control group.*

5.1.5 ADRB1, ADRB2, and ADRB3 protein expression in pancreatic islets

ADRB1 protein expression was not noticeably different between the HFSC and control groups (Figure 5), whereas *Adrb1* mRNA expression was elevated in the HFSC group. The expression levels of ADRB2 ($p < 0.01$) and ADRB3 ($p < 0.01$) proteins were significantly downregulated and upregulated, respectively, in the HFSC group compared with those in the control group.

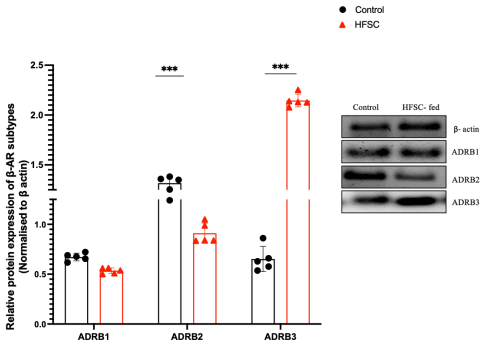

Figure 5. Effect of diet on β-adrenergic receptor (β-AR) subtype protein expression in mice.
*Data are expressed as mean ± standard deviation (SD) for five independent values. **p < 0.01 and ***p < 0.001 compared with the control group.*

5.1.6 β-AR localization in pancreas

Immunofluorescence analysis showed no significant changes in the localization of β1-AR in pancreatic islets under MetS conditions (Figure 6C, 6D). However, a notable decrease in β2-AR immunolocalization was observed in HFSC-fed mice compared to controls (Figure 6E, 6F). In contrast, β3-AR expression increased significantly in the HFSC group (Figure 6G, 6H). Quantitative analysis revealed no significant differences in β1-AR levels between the HFSC and control groups, while β2-AR expression significantly decreased ($p<0.01$) and β3-AR levels

significantly increased ($p<0.01$) in the HFSC group (Figure 7). These findings were consistent with western blot data, supporting the validity of our results.

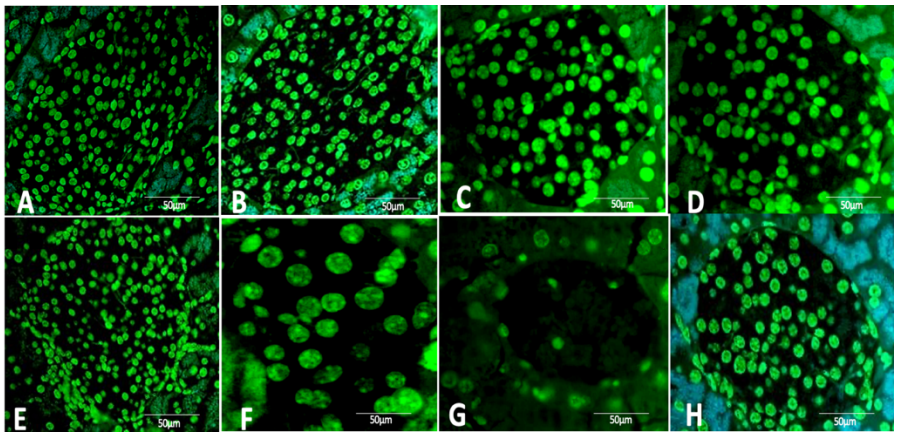

Figure 6. Immunofluorescence analysis of β-adrenergic receptor (β-AR) subtypes in mouse pancreatic islets.

Images at 400X magnification show (A) Control and (B) HFSC-fed samples with anti-β-actin antibody, (C) Control and (D) HFSC-fed samples with anti-β1-AR antibody, (E) Control and (F) HFSC-fed samples with anti-β2-AR antibody, (G) Control and (H) HFSC-fed samples with anti-β3-AR antibody

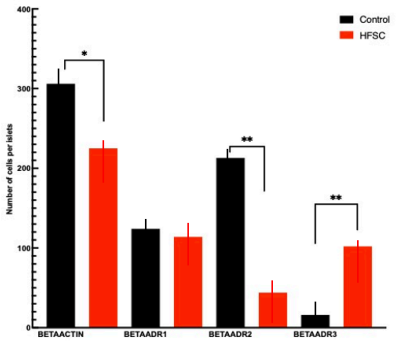

Figure 7. Immunofluorescence quantification of β-adrenergic receptor (β-AR) subtypes in mouse pancreatic islets.

*Analysis was performed using ImageJ (Fiji) and GraphPad Prism. The control and HFSC data represent measurements for each metabolic marker at different intervals. Data are expressed as mean ± SD for six independent values. **p < 0.01 and *p < 0.05 compared with the control.*

5.1.7 Intracellular cAMP concentration in pancreatic islets

The HFSC diet significantly altered intracellular cAMP levels in pancreatic islets compared to controls ($p< 0.01$, Figure 8), indicating a potential disruption in cAMP-dependent signaling

pathways within pancreatic islet cells. Cyclic nucleotide PDEs are key in intracellular signaling by breaking down cAMP and cyclic GMP. In HFSC-fed mice, low pancreatic cAMP levels boost PDE activity, hastening cAMP degradation and perpetuating reduced cAMP levels (Delhaye and Bardoni, 2021).

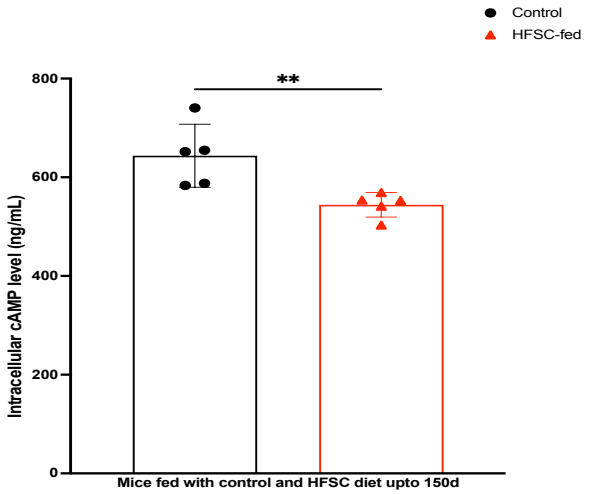

Figure 8. Effect of diet on cAMP levels in mice.

*Data are expressed as mean ± standard deviation (SD) for five independent values. **p < 0.01 compared to the control group.*

Although *Adrb1* levels were elevated in the HFSC group, no significant differences in ADRB1 expression were observed, which was further supported by reduced immunolocalization of β1-AR in islets from the HFSC group. This discrepancy suggests the possible involvement of translational regulatory mechanisms. The effect of HFSC diet on β2-AR expression indicates synchronized downregulation at both transcriptional and translational levels. The decrease in *Adrb2* levels corresponds to a reduction in ADRB2 expression, suggesting a finely tuned regulatory mechanism sensitive to dietary cues. Prolonged exposure to elevated levels of circulating catecholamines may reduce β-ARs (Schoken and Roth 1977) by desensitising these receptors *via* the protein kinase A pathway (Benovic 2002). The elevated norepinephrine levels in the plasma and hypothalamus of C57BL/6J mice (D'Souza and Abraham 2016) would have caused desensitisation of β2-AR (Nantel *et al.,* 1994). Despite stable *Adrb3* expression levels, heightened ADRB3 expression was observed in islets from HFSC diet-fed mice, suggesting potential post-transcriptional regulatory mechanisms enhancing ADRB3 protein upregulation in response to the HFSC diet. However, despite increased β3-AR abundance, pancreatic islets of HFSC diet-fed mice exhibited significantly reduced cAMP levels, indicating a dissociation between β3-AR and the cAMP signalling cascade. Although β1-AR expression remained unchanged, β2-AR expression decreased. The elevated β3-AR levels may compensate for the unchanged β1 and reduced β2-AR expression. Consequently, the increased β3-AR expression appears to have no discernible impact on cAMP levels, signifying a lack of functional influence within the cAMP signalling pathway despite its abundance.

5.2 PROTEOMIC PROFILE OF PANCREATIC ISLETS OF METS INDUCED C57BL/6J MICE

5.2.1 Differentially Expressed Proteins (DEPs)

Protein profiling using ESI-nanoLC-MS/MS identified 387 proteins in the pancreatic islets of both HFSC-fed and control groups of C57BL/6J mice. Protein identification was rigorously performed, requiring each protein to be represented by at least two peptides and one unique peptide. Data quality was enhanced through normalization using the MetaboAnalyst platform, addressing variability, outliers, and skewness. This normalization improved the consistency of the dataset, enabling more reliable identification of differentially expressed proteins. Principal Component Analysis (PCA) revealed a distinct separation between the control and HFSC groups, confirming the dietary effect on protein expression (Figure 9).

Further analysis, including volcano plot (Figure 10) and heatmap analysis (Figure 11), highlighted significant differences in protein expression between the groups. A total of 33 proteins were significantly upregulated in the HFSC group, suggesting that the diet positively influences their expression. Conversely, 34 proteins were downregulated in the HFSC group, indicating a reduction in their levels. The heatmap, combined with hierarchical clustering, showcased the distinct expression profiles between the two groups, with clustering revealing systematic patterns potentially driven by the dietary effects of the HFSC regimen.

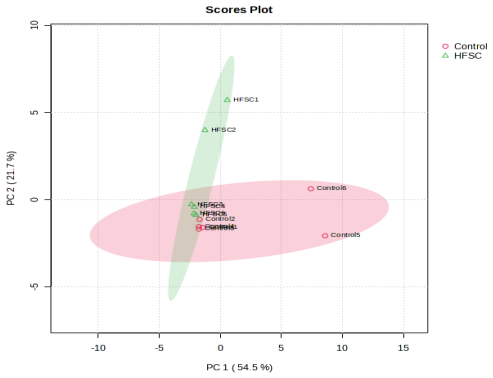

Figure 9. PCA Scores Plot: Clear separation between Control (red) and HFSC (green) groups, with distinct clusters and 95% confidence intervals.

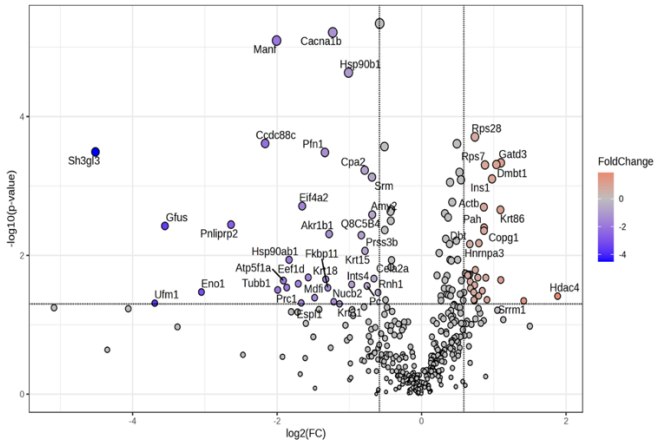

Figure 10. The volcano plot displays differentially expressed proteins in the HFSC group compared to the control group.

The x-axis represents the fold change (Log2 FC), while the y-axis represents each protein's statistical significance (-log10 q value). The student's t-test was used for analysis.

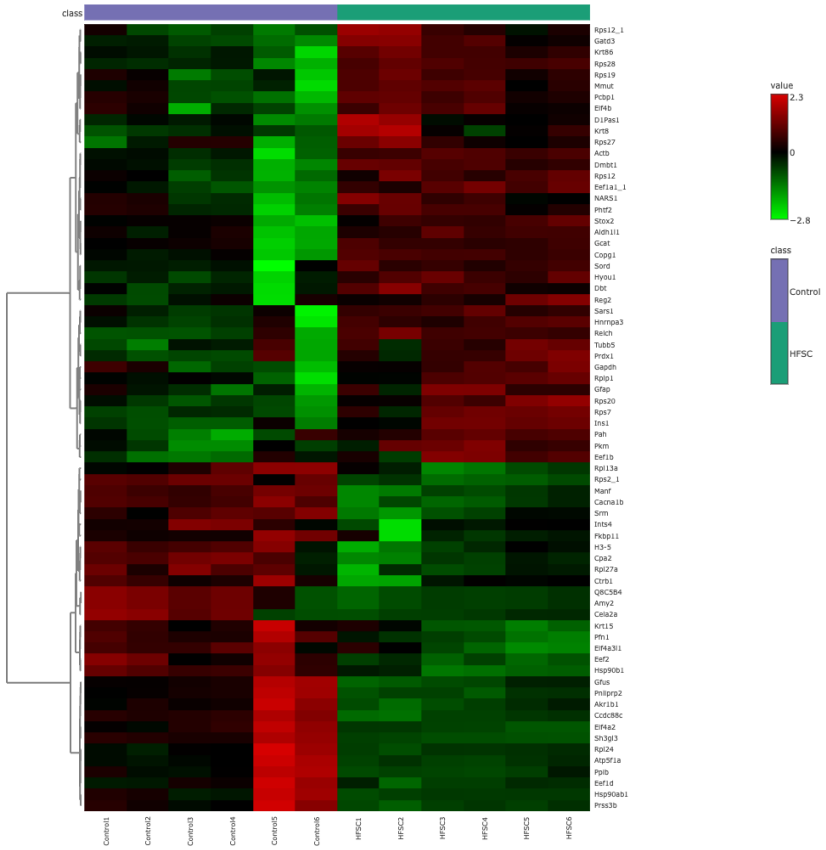

Figure 11. Heatmap represents data matrix of differentially expressed proteins in pancreatic islet of control and HFSC diet fed groups.

5.2.2 GO analysis : Biological process

Gene Ontology (GO) analysis of biological processes in the context of the HFSC diet revealed several key pathways involved in cellular stress response and metabolic adaptation (Figure 12). Notably, ribosomal small subunit assembly (GO:0000028) showed the highest fold enrichment (83.23), indicating an increased demand for ribosome biogenesis and protein synthesis machinery under metabolic stress conditions. Cytoplasmic translation (GO:0002181), with a fold enrichment of 31.80, suggests enhanced protein synthesis, likely as a compensatory response to the high-fat diet. Additionally, the process of protein folding (GO:0006457), enriched with a fold of 14.43, highlights the critical role of proper protein folding in managing the stress induced by metabolic alterations. Notably, the response to endoplasmic reticulum (ER) stress (GO:0034976) was also significantly enriched (9.82), pointing to the increased load of misfolded proteins requiring enhanced chaperone activity and cellular stress mechanisms. Lastly, the cellular response to stress (GO:0033554) (fold enrichment 3.13) reflects the broader mechanisms activated to cope with metabolic and oxidative stress, ensuring cellular homeostasis under the challenging conditions posed by the HFSC diet.

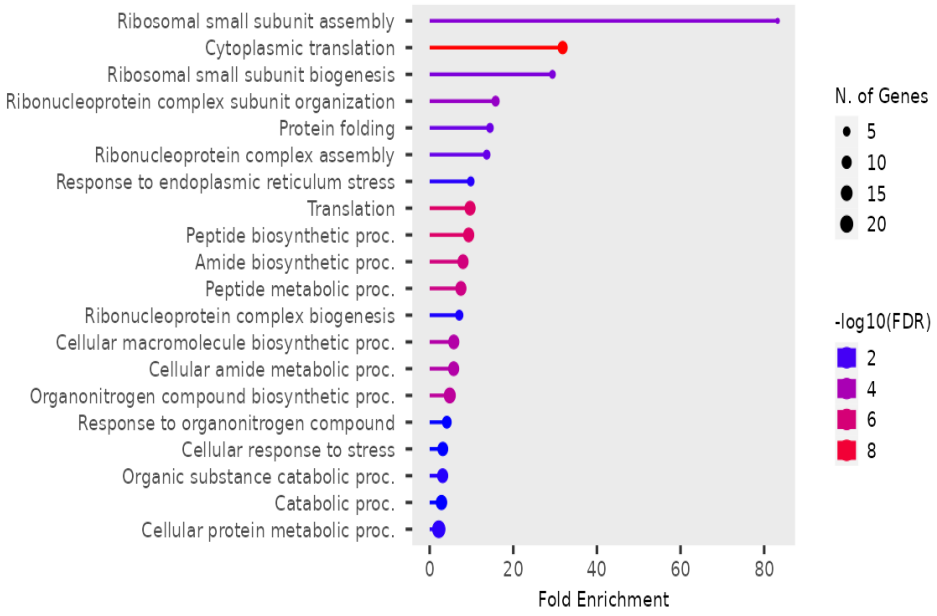

Figure 12. Gene Ontology (GO) analysis of differentially expressed proteins in pancreatic islets of mice fed HFSC diet compared with control

5.2.3 GO analysis :Cellular component

Gene Ontology (GO) analysis of cellular components in response to the HFSC diet highlighted several critical pathways involved in managing ER stress and maintaining cellular function under metabolic stress. The endoplasmic reticulum chaperone complex (GO:0034663) showed the highest fold enrichment (149.79), emphasizing the pivotal role of chaperones in managing ER stress. These chaperones facilitate proper protein folding and prevent the accumulation of misfolded proteins, which is essential for β-cells to meet the increased demand for insulin and maintain homeostasis during metabolic stress. The cytosolic small ribosomal subunit (GO:0022627), enriched at 63.74, underscores the importance of the protein synthesis

machinery in responding to metabolic disturbances, ensuring proper cellular function. Additionally, the endoplasmic reticulum lumen (GO:0005788), with a fold enrichment of 15.83, plays a key role in enhanced protein folding and stress responses, which are crucial for adapting to the HFSC-induced stress. Finally, the endoplasmic reticulum protein-containing complex (GO:0140534) enriched at 15.36 reflects the essential functions of ER complexes in protein folding, quality control, and stress adaptation, crucial for sustaining cellular function and adapting to the increased metabolic demands induced by a high-fat diet.

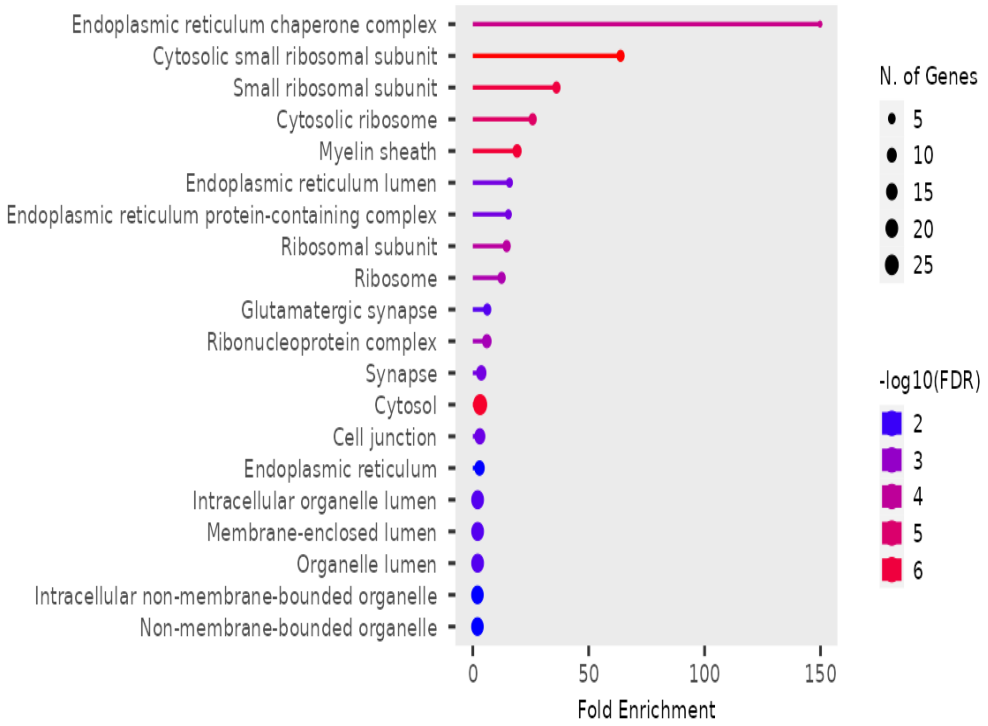

Figure 13. Gene Ontology (GO) analysis of differentially expressed proteins in pancreatic islets of mice fed HFSC diet compared with control.

5.2.4 GO analysis :Molecular function

Gene Ontology (GO) analysis of molecular functions in response to a high-fat diet (HFSC) identified key pathways associated with protein folding and cellular stress management. The ATP-dependent protein folding chaperone (GO:0140662) showed a significant fold enrichment of 62.41, indicating the crucial role of ATP-driven chaperones in managing protein folding, especially under stress induced by a high-fat diet. This process is essential for maintaining protein homeostasis and ensuring proper cellular function under metabolic stress. Additionally, the protein folding chaperone (GO:0044183) with a fold enrichment of 39.16 highlights the importance of chaperones in preserving protein stability and preventing aggregation, which is critical for cellular integrity during metabolic disturbances. These pathways are vital for adapting to the increased stress caused by a high-fat diet and maintaining the functionality of cellular machinery under challenging conditions.

Figure 14. Gene Ontology (GO) analysis of differentially expressed proteins in pancreatic islets of mice fed HFSC diet compared with control

5.2.5 KEGG pathway analysis

KEGG pathway analysis revealed several enriched pathways associated with metabolic changes in response to a HFSC diet. Notably, folate biosynthesis (fold enrichment 38.40) highlights a significant metabolic adaptation due to the dietary stress, indicating alterations in nucleotide metabolism. The pathway Type II diabetes mellitus (fold enrichment 31.20) suggests that HFSC diets induce changes in pancreatic islets that mirror those seen in the development of T2D, pointing to a potential mechanism for diet-induced metabolic dysfunction. Additionally, biosynthesis of amino acids (fold enrichment 19.20) reflects an increased demand for protein synthesis in pancreatic islets under dietary stress.

The protein processing in the endoplasmic reticulum (fold enrichment 17.62) pathway underscores the activation of mechanisms aimed at enhancing protein folding and managing ER stress in response to the HFSC diet, crucial for maintaining cellular function. Interestingly, the prostate cancer pathway (fold enrichment 15.13) was also enriched, possibly due to ER stress-induced by high-fat diets, triggering the unfolded protein response (UPR) in prostate cancer cells. Lastly, the amyotrophic lateral sclerosis (ALS) pathway (fold enrichment 6.83) highlights the potential connection between high-fat diets and neurodegenerative disease pathways, suggesting that the inflammatory and immune responses activated by the diet might contribute to cellular stress in pancreatic islets, potentially linking to ALS-like mechanisms.

The PPI network analysis reveals the critical role that heat shock proteins and chaperones, especially HSP90B1 and HSP90AB1, play in managing cellular stress and maintaining protein homeostasis, under a HFSC diet. These proteins are central to the cellular machinery that ensures proper protein folding, stress response, and survival when cells are subjected to metabolic stress. These findings highlight the complex molecular changes in pancreatic islets and suggest potential therapeutic targets for managing diet-induced metabolic disorders. Furthermore, the identification of pathways such as amyotrophic lateral sclerosis and prostate cancer suggests that high-fat diets could have broader implications for both metabolic and neurodegenerative diseases, indicating the need for further exploration of diet-induced cellular stress in these contexts.

5.3 HOMOLOGY MODELING AND MOLECULAR DOCKING OF MURINE β1-AR, β2-AR, AND β3-AR PROTEIN STRUCTURES

5.3.1 Structure prediction and validation of β-AR subtypes

The 3D structures of β1, β2, and β3-AR were predicted using Phyre 2, SWISS-MODEL, i-TASSER and AlphaFold. The best protein model was selected based on stereochemical analysis. The murine β-AR protein structure was predicted using the Phyre 2 and SWISS-MODEL tools. Phyre 2 was utilized to predict the optimal 3D structure for β1-AR and β3-AR proteins, while SWISS-MODEL specifically predicted the best structure for β2-AR. The stereochemical analysis of β1, β2, and β3-AR structures was conducted to validate their conformational quality for subsequent studies (Table 2). β1-AR exhibits a favorable Ramachandran plot distribution, with 83.1% of residues in the most favored regions, supported by an ERRAT score of 70.4225. However, the VERIFY3D score of 49.57% suggests areas for potential refinement. β2-AR demonstrates an even better Ramachandran plot distribution (89.1% in favored regions) and a higher ERRAT score of 80.3069, but a lower VERIFY3D score of 33.97%. β3-AR also shows a favorable Ramachandran plot distribution (93.2% in favored regions) with an ERRAT score of 93.4307, but a low VERIFY3D score of 15.60%, indicating areas for improvement.

5.3.2 Binding site identification and analysis

The identification of binding sites for β1-AR, β2-AR, and β3-AR involved predicting regions outside the transmembrane helices crucial for extracellular interactions. For β1-AR, these regions spanned amino acids 1-60, 118-131, 198-225, and 333-346; for β2-AR, amino acids 1-31, 90-108, 175-200, and 298-306 were identified; and for β3-AR, regions were found from amino acids 1-35, 94-107, 171-207, and 314-322. CASTp analysis revealed binding pockets inside the receptors. Experimental studies have identified specific residues such as Asp117, Ser209, Ser212, Ser169, Asn312, and Phe309 crucial for agonist binding in β3-ARs, and computational predictions closely match these findings, indicating agreement between computational and empirical data(Bowie *et al.,* 1991; Nagatomo *et al.,* 2001).

Table 2. Stereochemical analysis of β1-AR, β2-AR and β3-AR protein structure

	PROCHECK Ramachandran plot parameters-	**β1-AR (NP_031445.2)**	**β2-AR (NP_031446.2)**	**β3-AR (NP_038490.2)**
1	**Residues in most favoured regions [A,B,L]**	329 (83.1%)	334 (89.1%)	256(91.1%)
2	**Residues in additional allowed regions [a,b,l,p]**	52 (13.1%)	31 (8.3%)	20(7.1%)
3	**Residues in generously allowed regions [~a,~b,~l,~p]**	10 (2.5%)	7 (1.9%)	3(1.1%)
4	**Residues in disallowed regions**	5 (1.3%)	3 (0.8%)	2(0.7%)
5	**Number of non-glycine and non-proline residues**	396 (100.0%)	375 (100.0%)	281(100.0%)
6	**Number of end-residues (excl. Gly and Pro)**	2	2	3
7	**Number of glycine residues (shown as triangles)**	29	25	21
8	**Number of proline residues**	39	16	22
9	**Total number of residues**	466	418	327
10	**ERRAT**	70.4225	80.3069	85.938
11	**VERIFY 3D**	49.57%	33.97%	44.98%.

5.3.3 Molecular dynamic simulation

These plots derived from molecular dynamics (MD) simulations provide crucial insights into the stability, flexibility, and compactness of the murine β1, β2, and β3-adrenergic receptors over time (Figure 15, 16 and 17). RMSD plots for each receptor indicate rapid stabilization within the first 10 nanoseconds (ns), confirming that all three receptors quickly achieve stable conformations, with minimal structural deviations during the rest of the simulation. The RMSF plots highlight specific regions with higher flexibility, such as Pro 411 to Ser 412 for β1-AR and residues Gln 379 to Glu 380 for β2-AR, indicating areas likely crucial for ligand binding or functional dynamics. The Rg plots for β1 and β2-AR show a trend towards compactness, with β1-AR folding to a stable structure, while β2-AR maintains compactness, reflecting proper protein folding. For β3-AR, the Rg plot shows moderate fluctuations in compactness, suggesting some structural dynamics, yet the protein retains integrity over the 50 ns simulation period.

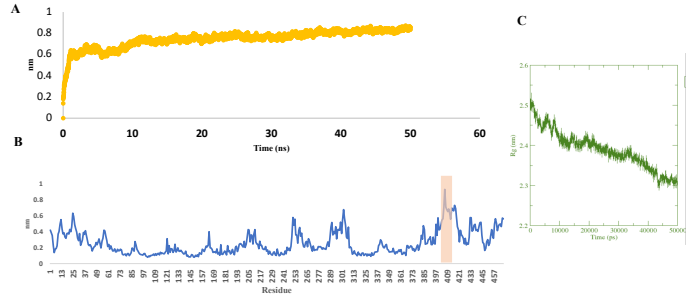

Figure 15. MD simulations analysis for murine β1-AR protein.
(A) RMSD study plot of murine β1-AR protein over 50 ns, (B) RMSF plot depicting the assessment of murine β1-AR, (C) Radius of Gyration plot reflecting the changes observed in the conformational behavior of murine β1-AR.

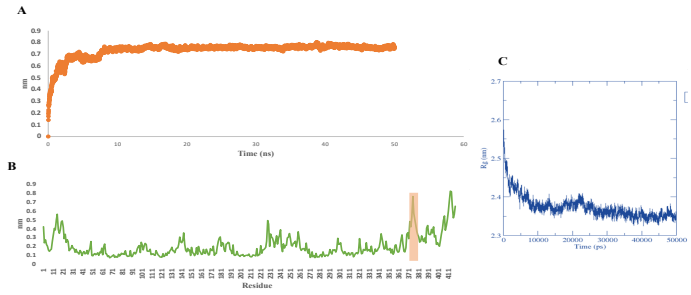

Figure 16. MD simulations analysis for murine β2-AR protein.
(A) RMSD study plot of murine β2-AR protein over 50 ns, (B) RMSF plot depicting the assessment of murine β2-AR, (C) Radius of Gyration plot reflecting the changes observed in the conformational behavior of murine β2-AR.

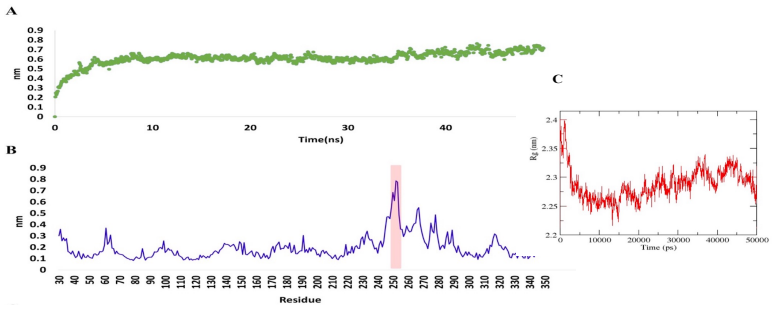

Figure 17. MD simulations analysis for murine β3-AR protein.
(A) RMSD study plot of murine β3-AR protein over 50 ns, (B) RMSF plot depicting the assessment of murine β3-AR, (C) Radius of Gyration plot reflecting the changes observed in the conformational behavior of murine β3-AR.

5.3.4 Analysis of binding interaction by molecular docking

Using molecular docking, the interaction between various ligands and β-adrenergic receptor (β-AR) subtypes was examined to elucidate their molecular basis. For β1-AR, NE exhibited a higher docking score of -5.8, forming a hydrogen bond with Thr93 (Figure 18A & 18B)). This indicates a stronger affinity of NE towards β1-AR. Propranolol showed a score of -5.2, suggesting alternative interactions may facilitate their association (Figure 19A & 19B). In β2-AR, NE achieved a score of -5.3, establishing three hydrogen bonds with crucial residues (Figure 20A & 20B). Propranolol demonstrated a stable interaction with a score of -5.7 (Figure 21A &21B). For β3-AR, NE scored -5.3 (Figure 22A & 22B), while CL316 243 showed a notably higher score of -7.2, forming a strong hydrogen bond (Figure 23A & 23B). L748 337 displayed a score of -6.4, with a significant hydrogen bond formed (Figure 24A & 24B). These findings provide valuable insights into the ligand-binding mechanisms of β-AR subtypes and their potential implications for drug design targeting metabolic and cardiovascular disorders.

A B

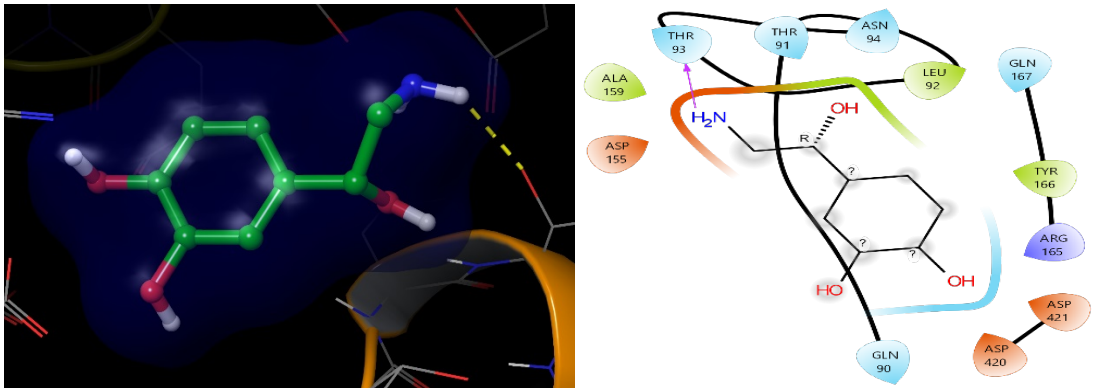

Figure 18. Molecular Docking Interaction of β1-AR. *(A) Pose view illustrating the interaction between Norepinephrine(NE) and β1-AR in the active site. (B) 2D interaction diagram showing the molecular docking between Norepinephrine(NE) and β1-AR.*

A B

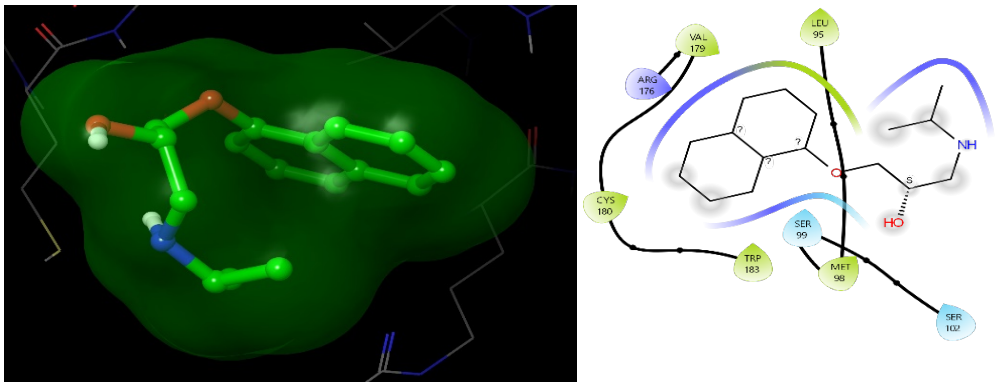

Figure 19. Molecular Docking Interaction of β1-AR. *(A) Pose view illustrating the interaction between Propranolol and β1-AR in the active site. (B) 2D interaction diagram showing the molecular docking between Propranolol and β1-AR.*

A B

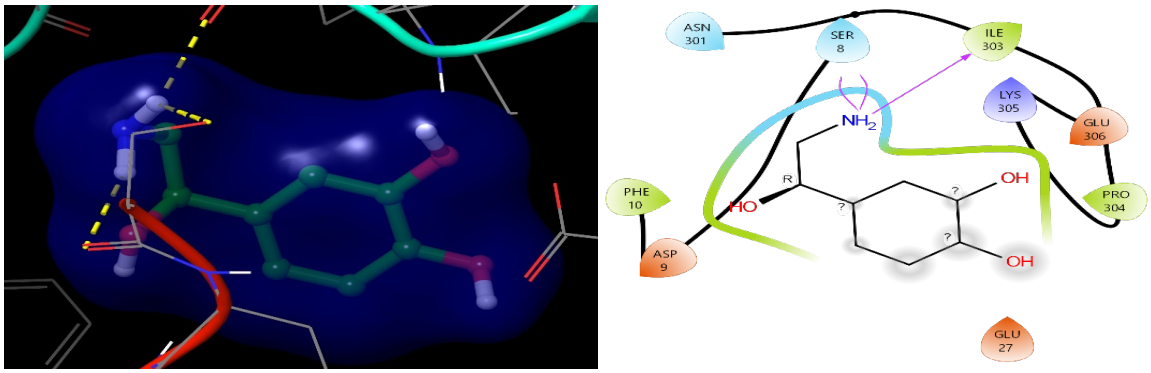

Figure 20. Molecular Docking Interaction of β2-AR. *(A) Pose view illustrating the interaction between Norepinephrine(NE) and β2-AR in the active site. (B) 2D interaction diagram showing the molecular docking between Norepinephrine(NE) and β2-AR.*

A B

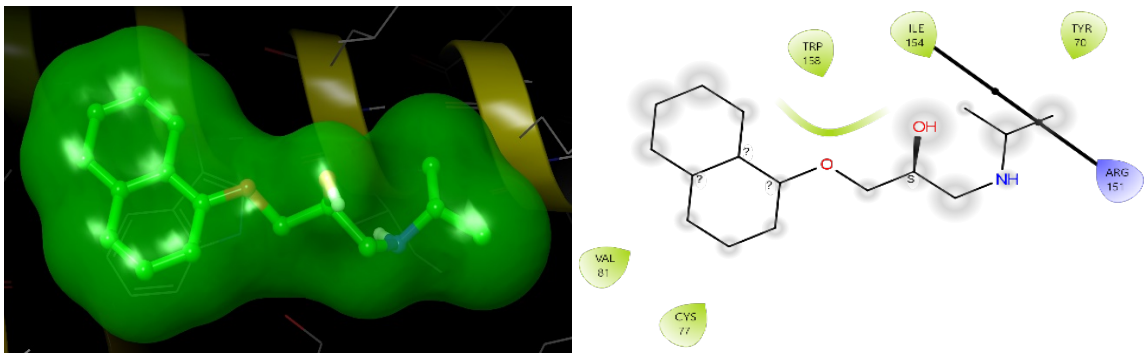

Figure 21. Molecular Docking Interaction of β2-AR. *(A) Pose view illustrating the interaction between Propranolol and β2-AR in the active site. (B) 2D interaction diagram showing the molecular docking between Propranolol and β2-AR.*

A B

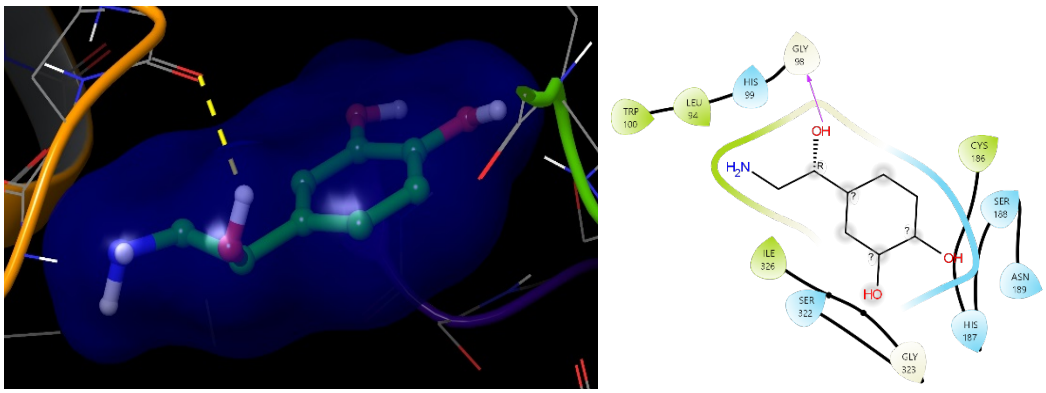

Figure 22. Molecular Docking Interaction of β3-AR. *(A) Pose view illustrating the interaction between Norepinephrine(NE) and β3-AR in the active site. (B) 2D interaction diagram showing the molecular docking between Norepinephrine(NE) and β3-AR.*

A B

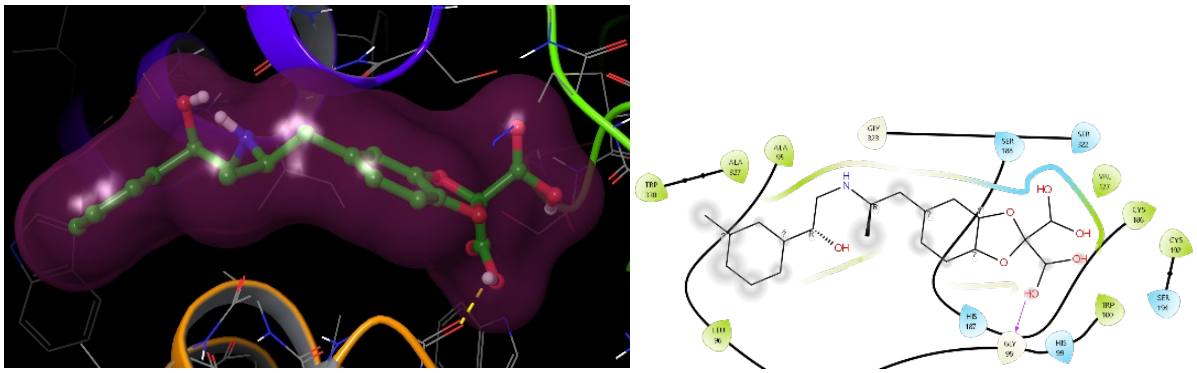

Figure 23. Molecular Docking Interaction of β3-AR. (*A) Pose view illustrating the interaction between CL316 243 and β3-AR in the active site. (B) 2D interaction diagram showing the molecular docking between CL316 243 and β3-AR.*

A B

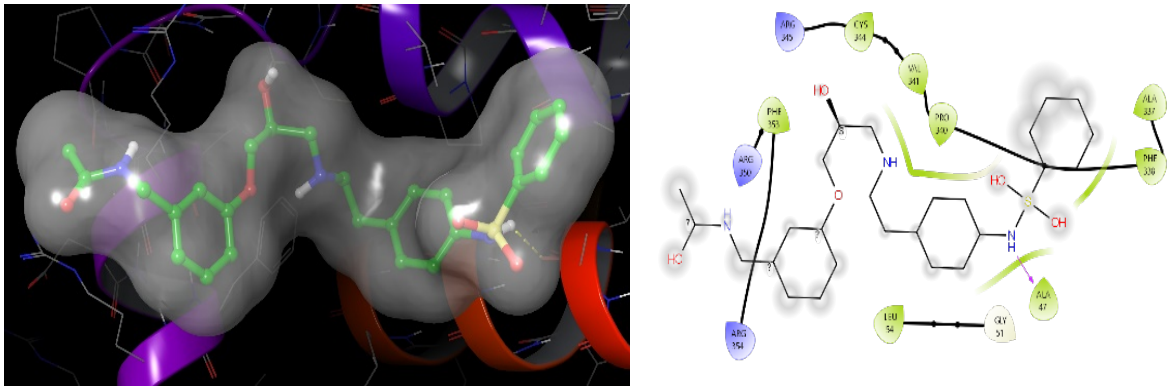

Figure 24. Molecular Docking Interaction of β3-AR. (A) *Pose view illustrating the interaction between L748 337and β3-AR in the active site. (B) 2D interaction diagram showing the molecular docking between L748 337and β3-AR.*

5. 4 INFLUENCE OF NE, β-AR AGONISTS, AND ANTAGONISTS ON GLUCOSE-INDUCED INSULIN SECRETION IN MICE PANCREATIC ISLETS

5.4.1 Glucose induced insulin secretion

Insulin secretion in isolated pancreatic islets was examined under normoglycemic (5mM) and hyperglycemic (20mM) conditions *in vitro*. Insulin levels were notably higher at 20mM glucose (284.914 µIU/mL) compared to 5mM glucose (201.1 µIU/mL), indicating a significant increase in secretion under hyperglycemic conditions (Figure 25).

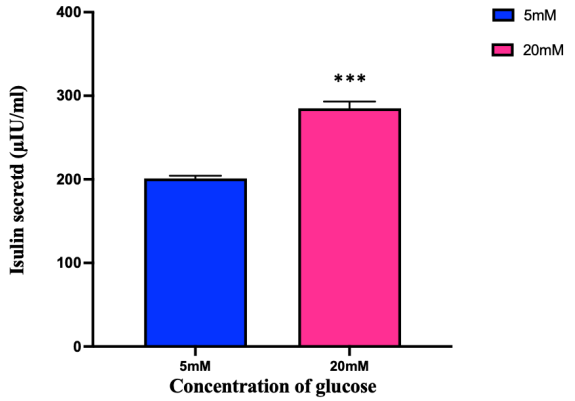

Figure 25. Glucose stimulated insulin secretion at low (5mM) and high (20mM) glucose concentration. *Data expressed as mean ± SD of 3 independent values. The graph was generated using GraphPad prism version 10.1*

5.4.2 Effect of NE on GIIS

We examined the impact of NE on insulin secretion under normoglycemic and hyperglycemic conditions. At normal glucose levels, NE did not significantly affect insulin secretion compared to the control. However, at a concentration of 100nM NE, insulin secretion notably increased ($p^{*}<0.05$) compared to control. Conversely, higher NE concentrations (1000nM and 10,000nM) suppressed insulin secretion. Intriguingly, under hyperglycemic conditions, NE consistently inhibited insulin secretion across all tested concentrations compared to the control (Figure 26).

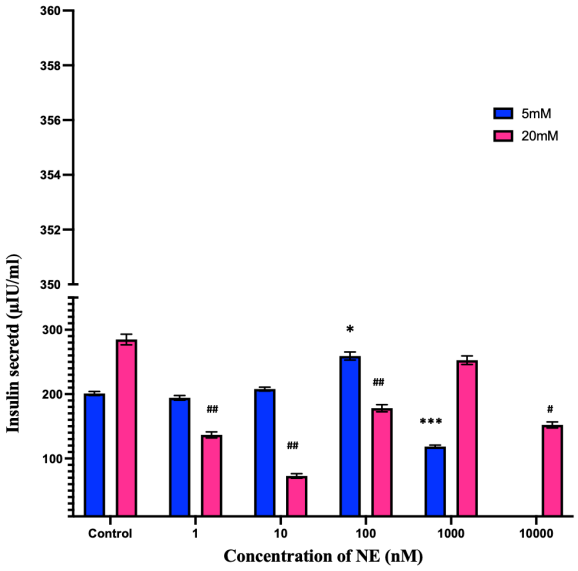

Figure 26. Effect of varying concentration of NE at low (5mM) and high (20mM) glucose induced insulin secretion.

Data expressed as mean ± SD of 3 independent values, $p^{***}<0.001$, $p^{*}<0.05$ when compared with 5mM control. $p^{\#\#}<0.01$, $p^{\#}<0.05$ when compared with 20mM control. The graph was generated using GraphPad prism version 10.1

5.4.3 Effect of β-AR agonist and antagonist on GIIS in presence of 100nM NE.

The role of β3-AR in insulin secretion was assessed by treating pancreatic islets with a β3-AR agonist, CL 316,243, in the presence of 100nM NE. Insulin secretion in response to CL 316,243 was observed under both conditions, though with lower levels (not significant) compared to controls. Blocking β3-AR with L748 337, a selective β3-AR antagonist, significantly decreased insulin secretion ($p^{**}<0.01$) under normal glucose conditions. Similarly, using propranolol, a nonselective β-AR antagonist, significantly decreased insulin secretion ($p^{**}<0.01$) at normal glucose levels but increased it at supraphysiological levels (Figure 27).

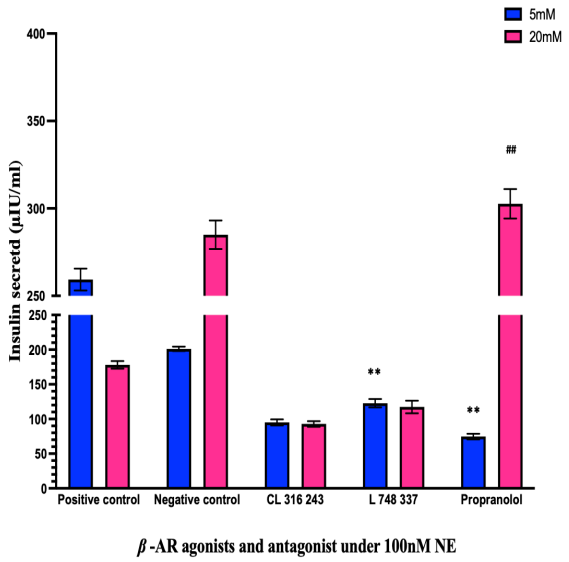

Figure 27. Effect of beta-adrenergic receptor agonist and antagonist in low (5mM) and high (20mM) glucose induced insulin secretion in presence of 100nM NE.

Data expressed as mean ± SD of 3 independent values. Negative control:5mM and 20mM glucose concentration, Positive control: 100nM NE in 5mM and 20mM glucose concentration , CL316 243: beta 3 adrenoceptor agonist, L748 337:beta 3 adrenoceptor antagonist and propranolol: a non-selective β-adrenergic receptor. All the antagonists were used at the concentration of 10nM, $p^{**}<0.01$ when compared with positive control at 5mM, $p^{\#\#}<0.01$ when compared with positive control at 20mM. The graph was generated using GraphPad prism version 10.1

5.4.4 Effect of β-AR agonist and antagonist on GIIS in presence of 10000nM NE.

To assess the chronic exposure of NE at 10,000 nM in the presence of β-AR agonists and antagonists on insulin secretion, we incubated pancreatic islets with the CL 316,243, L748 337, and propranolol (Fig. 12). CL 316,243 significantly increased insulin secretion under both normal ($p^{**}<0.01$) and hyperglycemic conditions ($p\#\#<0.01$) compared to the positive control.

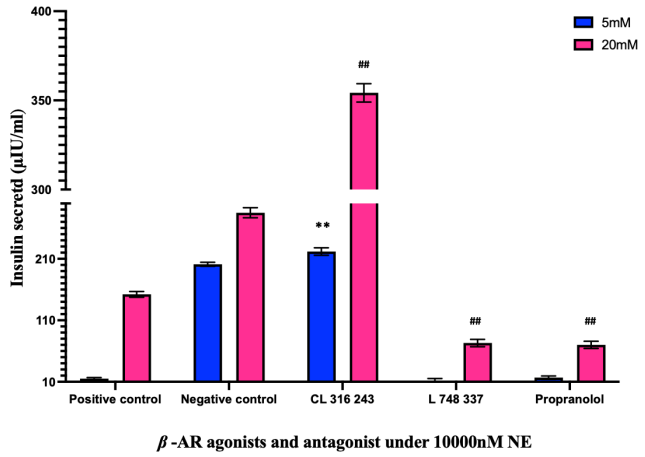

Figure 28. Effect of beta-adrenergic receptor agonist and antagonist in low (5mM) and high (20mM) glucose induced insulin secretion in presence of 10000nM NE.

*Data expressed as mean ± SD of 3 independent values. Negative control:5mM and 20mM glucose concentration, Positive control: 10000nM NE in 5mM and 20mM glucose concentration , CL316 243: beta 3 adrenoceptor agonist, L748 337:beta 3 adrenoceptor antagonist and propranolol: a non-selective β-adrenergic receptor. All the antagonists were used at the concentration of 10nM, p**<0.01 when compared with positive control at 5mM, $p^{\#\#}$<0.01 when compared with positive control at 20mM. The graph was generated using GraphPad prism version 10.1*

However, a significant decrease (*p##<0.01*) in insulin secretion was observed when using the L748 337, suggesting a significant role of β3-AR in mediating insulin secretion. In supraphysiological states, blocking both β1 and β2-AR using propranolol resulted in a significant decrease (*p##<0.01*) in insulin secretion (Figure 28). This indicates β3-AR plays a critical role in regulating insulin secretion, as evidenced by significant reductions in secretion upon β3-AR antagonism, suggesting its potential as a therapeutic target for insulin regulation.

6. SUMMARY AND FUTURE SCOPE

The investigation into the impact of an HFSC diet on expression of β1, β2, and β3-adrenergic receptors in pancreatic islets has provided insights into the intricate regulatory mechanisms affecting metabolic responses. Despite increased levels of *Adrb1*, no significant changes were observed in β1-AR protein expression. However, β2-AR expression decreased, suggesting a potential influence on glucose homeostasis and insulin secretion. Additionally, ADRB3 protein expression increased without affecting cAMP levels, indicating a lack of functional impact within the cAMP signaling pathway. Additionally, histopathological examination showed pancreatic steatosis, indicative of lipid accumulation and islet dysfunction. Disparities between gene and protein expression highlight the need for further exploration into post-transcriptional regulatory mechanisms, including miRNA involvement, translational control processes, and mRNA degradation.

This study provided a comprehensive proteomic analysis of pancreatic islets from mice on a HFSC diet, revealing substantial alterations in protein expression, including 387 identified proteins, many of which were differentially expressed. Key proteins such as HSP90B1, MANF,

and VCP were upregulated, playing critical roles in managing ER stress and protein folding, highlighting the adaptive response to dietary stress. Pathway analysis linked these changes to significant processes, including ribosomal biogenesis, T2D, chronic inflammation, and amino acid metabolism, suggesting a potential contribution to pancreatic ductal adenocarcinoma, metabolic disorders and neurodegenerative disorders like ALS. The identification of biomarkers like MANF and PRDX1 offers valuable insights into pancreatic cancer progression, suggesting their potential for early detection and therapeutic intervention. These findings underscore the molecular basis of metabolic dysregulation caused by high-fat diets and provide a foundation for future research on mitigating related risks.

Current study also provides a comprehensive analysis of the structural properties of the murine β-AR using advanced computational modelling techniques. Through theoretical assessments and comparative analyses of different modelling servers, we have gained valuable insights into the receptor's stability, conservation, and functional implications. Notably, Phyre and SWISS-MODEL emerges as a superior tools for accurately predicting the β2-AR's 3D structure, showcasing its ability to capture essential structural features with high fidelity.

Regarding the complex relationship between NE and insulin secretion, molecular docking studies revealed distinct interactions of NE and propranolol with β1-, β2-, and β3-ARs. NE exhibited a biphasic effect on insulin secretion under normal glucose levels, stimulating release at low concentrations but inhibiting it at higher concentrations. However, under hyperglycemic conditions, NE consistently inhibited insulin secretion. Differential effects of β3-AR agonist and antagonist on insulin secretion further underscored the significant role of β3-AR in mediating insulin secretion in mouse islets. Additionally, the non-selective β-AR antagonist propranolol showed varied effects on insulin secretion depending on glucose levels, possibly involving complex interactions with other signaling pathways.

7. PUBLICATIONS

1. Gangadhara V., Gawli K., and Abraham A. **Structural Insights into Mouse β3-Adrenergic Receptor: A Promising Target for Obesity and Diabetes Therapeutics** , (2024) *Letters in Drug Design and Discovery*. 10.2174/0115701808301580240405071948

2. Gangadhara V and Abraham A. **Primer Designing and Standardization of Primer Annealing Temperature for Beta-3-Adrenergic Receptor in *Mus Musculus.*** (2023), *International Journal of Pharmaceutical Sciences and Research*. doi: 10.13040/IJPSR.0975-8232.14(4).1934-39.

3. Gangadhara V and Abraham A. **Optimizing 3D Structural Predictions of Murine β2-Adrenergic Receptor: SWISS-MODEL Outperforms AlphaFold**: *Indian Journal of Pharmaceutical Education and Research* (ISSN-0019-5464*)* **(Decision pending).**

4. Gangadhara V and Abraham A. **Deciphering the involvement of Norepinephrine and β-Adrenergic Receptor subtypes in Glucose-induced Insulin Secretion: An Integrated *In Silico* and *In Vitro* Exploration using Isolated Pancreatic Islets of C57BL/6J Mice**. *Journal of Receptors and Signal Transduction.* (**Under Review).**

5. Gangadhara V., Gawli., K and Abraham A. **Discrepancies in β-Adrenergic Receptor Signalling and cAMP Pathway in High Fat Simple Carbohydrate diet-fed C57BL/6J mice: Implications for metabolic syndrome pathophysiology**. *Journal of Diabetes and its complications*. **Under review**

6. Gangadhara V and Abraham A. **Quantitative Proteomic Analysis of Mice Pancreatic Islets Reveals Diet-Induced Protein Expression Alterations and Signaling Pathway Changes Associated with Pancreatic Cancer Risk.** *Journal of Proteomics* **(Under review).**

8. PRESENTATIONS

1. Vijayalakshmi Gangadhara*, Bhagya N and Asha Abraham. **A Proteomic Study of Pancreatic Islets in Metabolic Syndrome-Induced Mice: Unravelling Dysregulated Pathways**, EMBL–Wellcome Connecting Science Conference: Proteomics in cell biology and disease mechanisms, EMBL Advanced Training Centre, Heidelberg, Germany, on 25 to 27 October 2023.
2. Vijayalakshmi Gangadhara* and Asha Abraham, "**Expression of beta-2 adrenergic receptors in the pancreatic islets of metabolic syndrome-induced C57BL/6J mice,"** at the 24th European Congress of Endocrinology, Milan, Italy, on May 21 to 24, 2022.
3. Vijayalakshmi Gangadhara* and Asha Abraham "**Effect of beta-adrenergic agonist and antagonist on glucose-induced insulin secretion *in vitro*"** during the 9th International Conference; 9th GDR3545 GPCR e-meeting, organised by Université de Tours, IFCE Centre INRAE Val de Loire 37380 Nouzilly, France, on November 6 to 9, 2020.
4. Vijayalakshmi Gangadhara* and Asha Abraham presented a paper titled "**Primer designing and *in-silico* PCR for beta-3-adrenergic receptor in *Mus musculus* C57BL/6J Strain**" at the International Conference on Advanced IT, Engineering, and Management held by AIMIT, St Aloysius College Mangalore, on November 21 to 22, 2019.

9. PRESENTATIONS/PUBLICATIONS (outside the thesis work)

- John JN, Mascarenhas RA, Gangadhara V, Abraham A. **Floral pigments and its cytotoxic activity: An update.** Indian Journal of Natural Products and Resources (IJNPR)[Formerly Natural Product Radiance (NPR)]. 2024 Apr 26;15(1):43-53.
- Jeffrina Nancy J., Rhea Ana Mascarenhas, Vijayalakshmi Gangadhara*, and Asha Abraham, "**Phytochemical screening and *in vitro* cytotoxic activity of floral pigments from *Callistephus chinensis*,"** at the National Conference organised by Vel Tech High Tech, Dr Ragaranjana, and Dr Sulekha Engineering College, Chennai, on June 10–11, 2022. **Won the 3rd Best Paper Award.**
- Rhea Ana Mascarenhas, Jeffrina Nancy J, Vijayalakshmi Gangadhara*, and Asha Abraham. "**Phytochemical screening and assessment of anti-oxidant and anti-mitotic activity of floral pigments from *Callistephus chinensis*"** at the National Conference on Phytocine organised by St Joseph College, Bangalore, on May 20-21, 2022.

- Mrinal M, Hemalatha Nambeeshan, Vijayalakshmi Gangadhara*, and Asha Abraham. "**Prediction of cardiovascular diseases using machine learning algorithms**" at the International Conference on Advanced IT, Engineering, and Management held by AIMIT at St Aloysius College Mangalore on December 2–3, 2021.
- Bhavya J. N., Manasvi, Vijayalakshmi Gangadhara*, and Asha Abraham "**Expression of PPAR isoforms in metabolic syndrome-induced C57BL/6J mice**," at the International Conference on Nurturing Innovative Technological Trends in Engineering Bioscience (NITTEBIO-2021), organised by NITTE, Karkala, Karnataka, on November 19-20, 2021**. Won Best paper award**.
- M. Jyothi Kumari, Vijayalakshmi Gangadhara*, and Asha Abraham "***In silico* assessment of selective alpha 2 adrenoreceptor antagonist over alpha 2 adrenergic receptor in *Mus musculus*"** at the International Conference on Nurturing Innovative Technological Trends in Engineering Bioscience (NITTEBIO-2021) organised by NITTE, Karkala, Karnataka, on November 19-20, 2021
- Pooja, Vijayalakshmi Gangadhara, and Asha Abraham "**Role of alpha-adrenergic receptors on glucose-induced insulin secretion *in vitro* using mouse pancreatic islets**" at the International Conference on Nurturing Innovative Technological Trends in Engineering Bioscience (NITTEBIO-2021), organised by NITTE, Karkala, Karnataka, on November 19-20, 2021.
- Bhavya J. N., Manasvi, Vijayalakshmi G*, and Asha Abraham presented a poster titled "**Standardisation of primer annealing temperature of PPAR gamma**" at the National Science Day event held at St. Aloysius College (autonomous) Mangalore on March 16, 2020. **Won the 2nd Best Poster Award**.
- Mrunal Damle, Pooja, Vijayalakshmi G*, and Asha Abraham presented a poster titled "**Standardisation and characterization of the MIN6 cell line *in vitro*"** at the National Science Day event held at St Aloysius College (autonomous) Mangalore on March 16, 2020. **Won the 3rd Best Poster Award.**
- Shreyoshree Mukherjee, Vijayalakshmi G*, and Asha Abraham presented a poster titled "**Primer designing and in silico PCR for thyroid hormone receptors"** at the National Conference on Current Advances in Medical and Industrial Biotechnology organised by Alvas College, Moodbidri, on February 20, 2020.

10. TRAINING/WORKSHOP ATTENDED

1) **Summer Internship Programme on Proteomics (Basic to Professional)** held between 1st May to 31st July, organized by IIT Bombay and Proteomic Intl Pvt Ltd.
2) **Workshop on "Computer Aided Drug Design"** held on 20th, 22nd, and 23rd July 2021, organized by the Research Directorate, NITTE (Deemed to be University) and Institutional Research Council, NGSMIPS, Nitte (DU), Mangaluru, in association with Schrödinger.
3) **Workshop on "Computer Aided Drug Designing – A Milestone in Drug Discovery"** organized by the Department of Pharmaceutical Chemistry, College of Pharmaceutical Sciences, Dayananda Sagar University, Bengaluru, on 9th April 2021.
4) **Workshop on "Untargeted Metabolomics using High Resolution Mass Spectrometry"** conducted by the Centre for Cellular and Molecular Platforms, Bangalore, held on 6th and 7th May 2020.
5) **Hands-on Training Workshop on "Basic Cell Culture Technology and Immunofluorescence"** held from 6th to 9th May 2019 at the National Centre for Cell Science, Pune.

6) **Hands-on training on the "Application of Biostatistics in Clinical Research"** conducted from 20th to 23rd February 2019, organized by NIMHANS, Bangalore.
7) **Hands-on training on "Realtime PCR"** conducted on 18th and 19th February 2019 by SRM University, Kanchipuram, Tamil Nadu.

11.REFERENCE

Aryal, N., Wasti, S.P., 2016. The prevalence of metabolic syndrome in South Asia: a systematic review. Int J Diabetes Dev Ctries 36, 255–262. https://doi.org/10.1007/s13410-015-0365-5

Asmat, U., Abad, K., Ismail, K., 2016. Diabetes mellitus and oxidative stress—A concise review. Saudi Pharm. J. 24, 547–553. https://doi.org/10.1016/j.jsps.2015.03.013

Borelli, M.I., Gagliardino, J.J., 2001. Possible modulatory effect of endogenous islet catecholamines on insulin secretion. BMC Endocr. Disord. 1, 1. https://doi.org/10.1186/1472-6823-1-1

Cai, Z., He, B., 2023. Adipose tissue aging: An update on mechanisms and therapeutic strategies. Metabolism 138, 155328. https://doi.org/10.1016/j.metabol.2022.155328

Cero, C., Lea, H.J., Zhu, K.Y., Shamsi, F., Tseng, Y.-H., Cypess, A.M., 2021. β3-Adrenergic receptors regulate human brown/beige adipocyte lipolysis and thermogenesis. JCI Insight 6, e139160. https://doi.org/10.1172/jci.insight.139160

Chatzigeorgiou, A., Halapas, A., Kalafatakis, K., Kamper, E., 2009. The use of animal models in the study of diabetes mellitus. In Vivo 23, 245–258.

Chen, M., Woods, S.C., Porte, D., 1975. Effect of Cerebral Intraventricular Insulin on Pancreatic Insulin Secretion in the Dog. Diabetes 24, 910–914. https://doi.org/10.2337/diab.24.10.910

Chu, D.-T., Malinowska, E., Jura, M., Kozak, L.P., 2017. C57BL/6J mice as a polygenic developmental model of diet-induced obesity. Physiol Rep 5, e13093. https://doi.org/10.14814/phy2.13093

D'Alessio, D., 2011. The role of dysregulated glucagon secretion in type 2 diabetes. Diabetes Obes. Metab. 13, 126–132. https://doi.org/10.1111/j.1463-1326.2011.01449.x

Dallongeville, J., Helbecque, N., Cottel, D., Amouyel, P., Meirhaeghe, A., 2003. The Gly ^{16} →Arg ^{16} and Gln ^{27} →Glu ^{27} Polymorphisms of β $_2$ -Adrenergic Receptor Are Associated with Metabolic Syndrome in Men. J. Clin. Endocrinol. Metab. 88, 4862–4866. https://doi.org/10.1210/jc.2003-030173

Delhaye, S., Bardoni, B., 2021. Role of phosphodiesterases in the pathophysiology of neurodevelopmental disorders. Mol. Psychiatry 26, 4570–4582. https://doi.org/10.1038/s41380-020-00997-9

Diane, A., Al-Shukri, N.A., Bin Abdul Mu-u-min, R., Al-Siddiqi, H.H., 2022. β-cell mitochondria in diabetes mellitus: a missing puzzle piece in the generation of hPSC-derived pancreatic β-cells? J. Transl. Med. 20, 163. https://doi.org/10.1186/s12967-022-03327-5

Dludla, P.V., Mabhida, S.E., Ziqubu, K., Nkambule, B.B., Mazibuko-Mbeje, S.E., Hanser, S., Basson, A.K., Pheiffer, C., Kengne, A.P., 2023. Pancreatic β-cell dysfunction in type 2 diabetes: Implications of inflammation and oxidative stress. World J. Diabetes 14, 130–146. https://doi.org/10.4239/wjd.v14.i3.130

D'Souza, S., Abraham, A., 2016. High-fat simple carbohydrate feeding impairs central and peripheral monoamine metabolic pathway triggering the onset of metabolic syndrome in C57Bl/6J mice. Neurol. India 64, 923–933. https://doi.org/10.4103/0028-3886.190261

DSouza, S.S., Abraham, A., 2019. High-fat simple carbohydrate (HFSC) diet impairs hypothalamic and corpus striatal serotonergic metabolic pathway in metabolic syndrome (MetS) induced C57BL/6J mice. Nutr. Neurosci. 22, 51–62. https://doi.org/10.1080/1028415X.2017.1354511

D'Souza, S.S., Abraham, A., 2014. A systematic study of biochemical profile during the induction and development of an animal model for Metabolic Syndrome. IOSR J. Pharm. Biol. Sci. 9, 109–113. https://doi.org/10.9790/3008-0914109113

D'Souza, S.S., Sri Charan Bindu, B., Mohammed Ali, M., Tisha, A., Deepthi, K.V., Siona, S., Santy, F., Abraham, A., 2016. Nutritional profile of High Fat Simple Carbohydrate Diet used to induce metabolic syndrome in C57BL/6J mice. J. Nutr. Intermed. Metab. 3, 41–49. https://doi.org/10.1016/j.jnim.2015.12.334

Esler, M., Straznicky, N., Eikelis, N., Masuo, K., Lambert, G., Lambert, E., 2006. Mechanisms of Sympathetic Activation in Obesity-Related Hypertension. Hypertension 48, 787–796. https://doi.org/10.1161/01.HYP.0000242642.42177.49

Fernandes, S., Severes, A., Kudnekar, T., Fernandes, A.C., Naik, D.R., Evan Dias, P., D'Souza, S., Abraham, A., 2015. High fat simple carbohydrate fed male Wistar rats: a useful model to study metabolic syndrome. Curr. Sci. 108, 1157–1165.

Fraulob, J.C., Ogg-Diamantino, R., Fernandes-Santos, C., Aguila, M.B., Mandarim-de-Lacerda, C.A., 2010. A Mouse Model of Metabolic Syndrome: Insulin Resistance, Fatty Liver and Non-Alcoholic Fatty Pancreas Disease (NAFPD) in C57BL/6 Mice Fed a High Fat Diet. J. Clin. Biochem. Nutr. 46, 212–223. https://doi.org/10.3164/jcbn.09-83

Fu, Z., R. Gilbert, E., Liu, D., 2013. Regulation of Insulin Synthesis and Secretion and Pancreatic Beta-Cell Dysfunction in Diabetes. Curr. Diabetes Rev. 9, 25–53. https://doi.org/10.2174/157339913804143225

Giacco, F., Brownlee, M., 2010. Oxidative Stress and Diabetic Complications. Circ. Res. 107, 1058–1070. https://doi.org/10.1161/CIRCRESAHA.110.223545

Gorain, B., Dutta, S., Nandy, U., Sengupta, P., Choudhury, H., 2020. Pharmacology of Adrenaline, Noradrenaline, and Their Receptors, in: Kumar, P., Deb, P.K. (Eds.), Frontiers in Pharmacology of Neurotransmitters. Springer Singapore, Singapore, pp. 107–142. https://doi.org/10.1007/978-981-15-3556-7_4

Gupta, R., Deedwania, P.C., Achari, V., Bhansali, A., Gupta, B.K., Gupta, A., Mahanta, T.G., Asirvatham, A.J., Gupta, S., Maheshwari, A., Saboo, B., Jali, M.V., Singh, J., Guptha, S., Sharma, K.K., 2013. Normotension, Prehypertension, and Hypertension in Urban Middle-Class Subjects in India: Prevalence, Awareness, Treatment, and Control. Am. J. Hypertens. 26, 83–94. https://doi.org/10.1093/ajh/hps013

Jha, B.K., Sherpa, M.L., Imran, M., Mohammed, Y., Jha, L.A., Paudel, K.R., Jha, S.K., 2023. Progress in Understanding Metabolic Syndrome and Knowledge of Its Complex Pathophysiology. Diabetology 4, 134–159. https://doi.org/10.3390/diabetology4020015

Jocken, J.W.E., Blaak, E.E., 2008. Catecholamine-induced lipolysis in adipose tissue and skeletal muscle in obesity. Physiol. Behav. 94, 219–230. https://doi.org/10.1016/j.physbeh.2008.01.002

Kasuga, M., 2006. Insulin resistance and pancreatic beta cell failure. J Clin Invest 116, 1756–1760. https://doi.org/10.1172/JCI29189

Kojima, I., Medina, J., Nakagawa, Y., 2017. Role of the glucose-sensing receptor in insulin secretion. Diabetes Obes. Metab. 19, 54–62. https://doi.org/10.1111/dom.13013

Lacey, R.J., Berrow, N.S., London, N.J.M., Lake, S.P., James, R.F., Scarpello, J.H.B., Morgan, N.G., 1990. Differential effects of β-adrenergic agonists on insulin secretion from pancreatic islets isolated from rat and man. J. Mol. Endocrinol. 5, 49–54. https://doi.org/10.1677/jme.0.0050049

Lee, M.-W., Lee, M., Oh, K.-J., 2019. Adipose Tissue-Derived Signatures for Obesity and Type 2 Diabetes: Adipokines, Batokines and MicroRNAs. J. Clin. Med. 8, 854. https://doi.org/10.3390/jcm8060854

Li, R., Huang, H., Limesand, S.W., Chen, X., 2021. Pancreatic Islets Exhibit Dysregulated Adaptation of Insulin Secretion after Chronic Epinephrine Exposure. Curr. Issues Mol. Biol. 43, 240–250. https://doi.org/10.3390/cimb43010020

Martinez-Sanchez, N., Sweeney, O., Sidarta-Oliveira, D., Caron, A., Stanley, S.A., Domingos, A.I., 2022. The sympathetic nervous system in the 21st century: Neuroimmune interactions in metabolic homeostasis and obesity. Neuron 110, 3597–3626. https://doi.org/10.1016/j.neuron.2022.10.017

Masuo, K., 2010. Roles of Beta2- and Beta3-Adrenoceptor Polymorphisms in Hypertension and Metabolic Syndrome. Int. J. Hypertens. 2010, 1–12. https://doi.org/10.4061/2010/832821

Nagiri, C., Kobayashi, Kazuhiro, Tomita, A., Kato, M., Kobayashi, Kan, Yamashita, K., Nishizawa, T., Inoue, A., Shihoya, W., Nureki, O., 2021. Cryo-EM structure of the β3-adrenergic receptor reveals the molecular basis of subtype selectivity. Mol. Cell 81, 3205-3215.e5. https://doi.org/10.1016/j.molcel.2021.06.024

Nestel, P.J., Khan, A.A., Straznicky, N.E., Mellett, N.A., Jayawardana, K., Mundra, P.A., Lambert, G.W., Meikle, P.J., 2017. Markers of sympathetic nervous system activity associate with complex plasma lipids in metabolic syndrome subjects. Atherosclerosis 256, 21–28. https://doi.org/10.1016/j.atherosclerosis.2016.11.032

Paranjape, S.A., Chan, O., Zhu, W., Horblitt, A.M., McNay, E.C., Cresswell, J.A., Bogan, J.S., McCrimmon, R.J., Sherwin, R.S., 2010. Influence of Insulin in the Ventromedial Hypothalamus on Pancreatic Glucagon Secretion In Vivo. Diabetes 59, 1521–1527. https://doi.org/10.2337/db10-0014

Prentki, M., Nolan, C.J., 2006. Islet cell failure in type 2 diabetes. J. Clin. Invest. 116, 1802–1812. https://doi.org/10.1172/JCI29103

Rasmussen, S.G.F., Choi, H.-J., Rosenbaum, D.M., Kobilka, T.S., Thian, F.S., Edwards, P.C., Burghammer, M., Ratnala, V.R.P., Sanishvili, R., Fischetti, R.F., Schertler, G.F.X., Weis, W.I., Kobilka, B.K., 2007. Crystal structure of the human β2 adrenergic G-protein-coupled receptor. Nature 450, 383–387. https://doi.org/10.1038/nature06325

Rodrigues, A.C., Prímola-Gomes, T.N., Peluzio, M.C.G., Hermsdorff, H.H.M., Natali, A.J., 2021. Aerobic exercise and lipolysis: A review of the β-adrenergic signaling pathways in adipose tissue. Sci. Sports 36, 16–26. https://doi.org/10.1016/j.scispo.2020.04.006

Roh, E., Song, D.K., Kim, M.-S., 2016. Emerging role of the brain in the homeostatic regulation of energy and glucose metabolism. Exp Mol Med 48, e216–e216. https://doi.org/10.1038/emm.2016.4

Roy, N., 2020. Analysis of adrenergic receptors during the onset and progression of metabolic syndrome (PhD Thesis). Mangalore University.

Sakamoto, Y., Oniki, K., Kumagae, N., Morita, K., Otake, K., Ogata, Y., Saruwatari, J., 2019. *Beta-3-adrenergic Receptor* rs4994 Polymorphism Is a Potential Biomarker for the Development of Nonalcoholic Fatty Liver Disease in Overweight/Obese Individuals. Dis. Markers 2019, 1–13. https://doi.org/10.1155/2019/4065327

Samsonova, N.G., Zvenigorodskaia, L.A., 2011. [Pancreas and metabolic syndrome]. Eksp Klin Gastroenterol 68–72.

Schiffelers, S., 2000. In vivo β3-adrenergic stimulation of human thermogenesis and lipid use. Clin. Pharmacol. Ther. 67, 558–566. https://doi.org/10.1067/mcp.2000.106794

Straub, S.G., Sharp, G.W.G., 2012. Evolving insights regarding mechanisms for the inhibition of insulin release by norepinephrine and heterotrimeric G proteins. Am. J. Physiol.-Cell Physiol. 302, C1687–C1698. https://doi.org/10.1152/ajpcell.00282.2011

Swarnalatha, B.N., D Souza Sthephen, S., Abraham, A., 2016. Insulin resistance precedes glucose intolerance and hyperleptinaemia in high-fat simple carbohydrate-fed C57BL/6J mice. Endokrynol. Pol. 67, 592–598. https://doi.org/10.5603/EP.2016.0069

Swarnalatha, N.B., Roy, N., Gouda, M.M., Moger, R., Abraham, A., 2018. High-fat, simple-carbohydrate diet intake induces hypothalamic–pituitary–thyroid axis dysregulation in C57BL/6J male mice. Appl. Physiol. Nutr. Metab. 43, 371–380. https://doi.org/10.1139/apnm-2017-0410

Thorp, A.A., Schlaich, M.P., 2015. Relevance of Sympathetic Nervous System Activation in Obesity and Metabolic Syndrome. J. Diabetes Res. 2015, 1–11. https://doi.org/10.1155/2015/341583

Walker, J.N., Ramracheya, R., Zhang, Q., Johnson, P.R.V., Braun, M., Rorsman, P., 2011. Regulation of glucagon secretion by glucose: paracrine, intrinsic or both? Diabetes Obes. Metab. 13, 95–105. https://doi.org/10.1111/j.1463-1326.2011.01450.x

Warne, T., Serrano-Vega, M.J., Baker, J.G., Moukhametzianov, R., Edwards, P.C., Henderson, R., Leslie, A.G.W., Tate, C.G., Schertler, G.F.X., 2008. Structure of a β1-adrenergic G-protein-coupled receptor. Nature 454, 486–491. https://doi.org/10.1038/nature07101

Zaqout, S., Becker, L.-L., Kaindl, A.M., 2020. Immunofluorescence Staining of Paraffin Sections Step by Step. Front. Neuroanat. 14, 582218. https://doi.org/10.3389/fnana.2020.582218